Machine Learning
Data Analytics

Friedrich-Alexander-Universität
Technische Fakultät

EmpkinS

Machine Learning-Based Detection of Acute Psychosocial Stress from Dynamic Movements

Master's Thesis in Medical Engineering

submitted
by

Luca Abel

born 27.02.1996 in Malsch

Written at

Machine Learning and Data Analytics Lab
Department Artificial Intelligence in Biomedical Engineering
Friedrich-Alexander-Universität Erlangen-Nürnberg (FAU)

in Cooperation with

Chair of Health Psychology
Friedrich-Alexander-Universität Erlangen-Nürnberg (FAU)

Advisors:	Robert Richer M.Sc., Arne Küderle M.Sc., Prof. Dr. Bjoern Eskofier, Prof. Dr. Nicolas Rohleder (Chair of Health Psychology)
Started:	01.12.2021
Finished:	01.06.2022

Ich versichere, dass ich die Arbeit ohne fremde Hilfe und ohne Benutzung anderer als der angegebenen Quellen angefertigt habe und dass die Arbeit in gleicher oder ähnlicher Form noch keiner anderen Prüfungsbehörde vorgelegen hat und von dieser als Teil einer Prüfungsleistung angenommen wurde. Alle Ausführungen, die wörtlich oder sinngemäß übernommen wurden, sind als solche gekennzeichnet.
Die Richtlinien des Lehrstuhls für Bachelor- und Masterarbeiten habe ich gelesen und anerkannt, insbesondere die Regelung des Nutzungsrechts.

Erlangen, den 01.06.2022

Übersicht

Stress ist einer der wichtigsten Faktoren, der die menschliche Gesundheit beeinflusst. Die Auswirkungen von Stress wurden bisher in erster Linie mit Hilfe von Blut- und Speichelbiomarkern wie Cortisol, Amylase, Entzündungsmarkern, sowie elektrophysiologischen Messungen und Selbstberichten untersucht. Diese Methoden liefern ein relativ gutes Maß für die Auswirkungen von Stress auf den Körper und damit auf die Gesundheit. Jedoch sind diese etablierten Messmethoden teuer, arbeitsintensiv, nur begrenzt skalierbar und nur im Labor voll anwendbar. Ein vielversprechender Ansatz, um diese Maßnahmen kurzfristig zu ergänzen und langfristig vollständig zu ersetzen, ist die Beobachtung von Körperbewegungen zur Stressbewertung.

Um einen ersten Schritt in Richtung berührungslose Stresserkennung zu unternehmen, wurde eine Studie durchgeführt, in der Körperhaltung und -bewegung mit einem Motion-Capture-System während einer akuten Stresssituation gemessen wurde. Einundvierzig Teilnehmer wurden an zwei aufeinanderfolgenden Tagen dem Trier Social Stress Test (TSST) und der stress-freien Kontrollbedingung, dem friendly Trier Social Stress Test (f-TSST) in einer zufälligen Reihenfolge ausgesetzt. Die Bewegungsdaten wurden sowohl während des (f-)TSST als auch während standardisierter Gang- und Bewegungstests aufgezeichnet, um die Auswirkungen von Stress auf dynamische Bewegungen zu erforschen. Aus den Motion-Capture-Daten wurden verschiedene Bewegungsmerkmale abgeleitet, die statistisch ausgewertet wurden. Wie aus vorhergehenden Arbeiten zu erwarten war, zeigten die Teilnehmer während des TSST ein defensives “Freezing”-Verhalten, das durch eine reduzierte Kopf-, Hand-, Brust- und Ganzkörperbewegung quantifiziert werden konnte. Die Ergebnisse der Gang- und Bewegungstests zeigten keinen Einfluss der Stresssituation im Vergleich zur Kontrollbedingung.

Um festzustellen, ob Körperbewegungen die etablierten Stressmessgrößen wie Cortisol oder Selbstberichte zuverlässig vorhersagen können, wurde eine Regressionsanalyse durchgeführt. Mit diesem Ansatz konnten 60 % der Varianz des maximalen relativen Cortisolanstiegs erklärt werden. Darüber hinaus wurde ein Klassifikator trainiert, um anhand von Bewegungsmerkmalen zwischen Stress- und Nichtstressbedingungen zu unterscheiden, wobei eine Genauigkeit von 74,3 $\pm$ 4,2 % erreicht wurde. Desweiteren wurde eine ML-basierte Regression zur Vorhersage des maximalen relativen Cortisolanstiegs sowie von Selbstberichten zu Herausforderung und Bedrohung verwendet, wobei sich herausstellte, dass diese Werte allein durch Bewegungsmerkmale nicht mit hoher Genauigkeit vorhergesagt werden können.

Abstract

Stress is one of the most important factors influencing human health. The effects of acute stress have been studied primarily using blood and saliva biomarkers such as cortisol, alpha-amylase (α-amylase), inflammatory markers, electrophysiological measures, and self-reports. To date, these methods provided a relatively good measure of the effects of stress on the body and thus on health. However, these established measures are expensive, labor-intensive, have limited scalability, and are only fully applicable in the laboratory. A promising approach to supplement these measures in the short term and replace them completely in the long term can be provided by observing body movements for stress assessment.

To make a step towards contactless stress detection, a study measuring body posture and movement with a motion capture system during an acute stress situation was conducted within the scope of this thesis. Fourty-one participants were exposed to the Trier Social Stress Test (TSST) and the friendly Trier Social Stress Test (f-TSST) in randomized order on two consecutive days. Motion capture data were recorded both during the (f-)TSST, as well as during standardized gait and mobility tests to assess the impact of stress on dynamic movements. Various motion features were derived from the motion capture data, which were statistically analyzed. As expected from previous work, participants showed a defensive freezing behavior during the TSST, quantified by reduced head, hand, chest, and total body motion. Results from the gait and mobility tests showed no impact of acute psychosocial stress compared to the control condition.

To assess if body motions can reliably predict the well-established stress measures, such as salivary cortisol or self-reported levels of perceived stress, a stepwise backward multiple linear regression was performed. With this approach, 60 % of the variance of the maximum relative cortisol increase, could be explained. Furthermore, a machine learning model was trained to differentiate between the stress and non-stress conditions by motion features, with achieved an accuracy of 74.3 ± 4.2 %. Additionally, ML-based regression was used to predict the maximum relative cortisol increase, as well as self-report measures of challenge and threat, which revealed that these measures cannot be predicted accurately by motion features only.

Contents

Chapter 1

Introduction

Stress is universally present in all our daily lives. Although stress is a healthy reaction of our body, extensive stress can severely affect health and mental wellbeing [OCo21]. For this reason, stress is now recognized as a major cause of long-term illness in many countries around the world [APA19; Pol21], in addition to being associated with a variety of diseases, including life-threatening conditions such as cardiovascular disease, insulin insensitivity, and cancer [Coh07].

On a biological level, various neuroendocrine responses occur in response to stress. The two most important stress signaling pathways are the sympathetic nervous system (SNS) and hypothalamic-pituitary-adrenal (HPA) axis. The SNS is responsible for the "fight-or-flight" response in emergency conditions. These are responsible, among other things, for the release of the well-established stress markers: α-amylase and cortisol [Ulr09]. Cortisol is most specific activation marker of HPA axis for acute psychological stress response [Fol10].

Despite the fact that stress and its effects have been researched extensively, the standard method of measuring neuroendocrine and electrophysiological markers requires a significant amount of effort on the part of researchers. Furthermore, typical assessment approaches are often invasive, particularly when measuring the inflammatory response triggered in response to acute stress [Roh19] and can only be accurately quantified via blood samples [Sla15]. Even when noninvasive methods are used, they require at least some interference with natural human behavior [Kaz79].

Thus, there is a need to develop novel, non-invasive, potentially contactless, measurement modalities. One possibility of contactless monitoring of stress reactions might be given by observing bodily motions and posture. Several studies have reported defensive freezing behavior in response to acute stress [Roe10; Hag14]. Dynamic movements, such as walking, can provide even more information about stress-related changes in movement patterns that are not visible in static poses.

Previous work has shown that several mental and physical illnesses can be linked to distinct variations of gait and body posture. For instance, patients suffering from depression had a slower gait and slumped posture [Fel20]. Lasselin et al. showed that acute systemic inflammation can be connected to gait and posture alterations [Las20]. Hence, it is expected that similar gait and postural changes can be observed following a stressful event.

The goal of this master's thesis is, therefore, to extend the knowledge about how acute stress can be unobtrusively measured from body posture and movements. To achieve that, a randomized cross-over study was conducted as a part of the EmpkinS collaborative research center [Emp22]. As part of this study, the participants performed the TSST [Kir93] and the f-TSST [Wie13] in randomized order on two consecutive days. The TSST is the gold standard for inducing acute psychosocial stress in a laboratory setting designed like a mock job interview, whereas the f-TSST is used as a control condition with a similar mental demand that should not elicit a stress response.

In addition to the traditional stress markers, IMU-based motion capture (MoCap) data were recorded during the stress exposure as well as during standardized gait and mobility tests which were performed before and after the stress task. The gait and mobility tests included the Timed Up & Go (TUG) [Pod91] protocol as well as 4×10 m walking tests.

The recorded MoCap data were used to calculate various parameters, which were then statistically analyzed. A backward multiple linear regression was used to examine the relationship between bodily motions and traditional stress markers cortisol and salivary α-amylase (sAA), assessed via saliva samples, as well as self-reported levels of stress, anxiety, and threat, assessed via questionnaires. In addition, machine learning (ML) models were trained and evaluated with the aim of distinguishing stressed from non-stressed participants and predicting biological stress responses.

Chapter 2

Related Work

Observing body posture and movements can give various insights about the physical and psychological state of an individual. While humans have the natural ability to recognize if someone is sick, angry, frightened, or anxious, objective and unobtrusive measuring of these inner states is an ongoing research task [Cal14; Sar19; Bid20].

Emotion Recognition

Previous work showed that negative and positive emotions can be detected from body posture and movements. Research using point light displays (PLDs), which are simple projections that reduce the movement of the human body to points of light at a few defined locations, revealed that people are able to infer the emotions of other individuals just from the movements of these point lights. In the work of Atkinson et al. the emotions anger, disgust, fear, happiness, and sadness could be reliably detected by the participants from PLDs [Atk04].

Boone and Cunningham reported the following six movement cues used by participants for the perception of affect-expressive dance movements: changes in tempo (anger), directional changes in face and torso (anger), frequency of arms up (happiness), duration of arms away from torso (happiness), muscle tension (fear), and the duration of time leaning forward (sadness) [Boo98].

Camurri et al. suggest that the movement duration and quantity (i.e., the amount of observed movement relative to the velocity and movement energy represented), as well as the contraction index (measured as the amount of body contraction/expansion) are important for the perception of affect from dance movements [Cam04].

With the facial action coding system (FACS), Ekman et. al. have established a system for describing facial expressions by extracting activations of certain muscle groups in the face (so-called action units) and composing them into basic emotions [Ekm78]. Up to now, only one study investigated the facial expressions of healthy female subjects in the TSST [Lup14]. The results indicated that the expressions of both fear and anger were associated with the cortisol response to the TSST.

Van der Zee et al. used motion capturing to record the full-body movement of participants while lying or telling the truth. Half of their study group were instructed to lie. For comparing the full-body movement they calculated the absolute movement of the whole participant's body, which is defined as the sum of joint displacement between two samples. Their findings suggested that liars tend to move around more compared to the control group. They were also able to correctly classify 74.4% of the participants as either truth-tellers or liars utilizing a two-predictor binary logistic regression [Zee19].

Bodily Movements & Stress

One possible reaction of the human body due to acute stress, that has been observed in multiple studies, is freezing. Freezing is one of the best-known defensive responses of animals to the threat of predators. It is characterized by reduced body movements and a decreased heart rate compared to pre-threat levels [Bla86]. Defensive freezing behavior similar to that seen in animals can also be observed in humans. Roelofs et al. conducted a study with 50 participants, where socially threatening viewing cues (angry faces) were shown to them. Their results suggest that body sway was significantly reduced in comparison to the control condition [Roe10]. In a follow up work, Haagenars et al. observed freezing-like responses as a response to unpleasant films [Hag14]. Despite the potential importance of freezing for human stress detection and management, its phenomenology basis remains largely unexplored in humans [Roe17]. One study by Gladwin et al. investigated whether freezing is an active or passive preparatory state, by measuring body sway with a stabilometric force platform. They concluded that freezing is an active preparation for a possible fight or flight response, since it is strongly related to the ability to respond [Gla16]. In a study by Hashemi et al., individual differences in anticipatory freezing responses could be predicted by accumulated hair cortisol concentrations and anxiety characteristics. The study population was a mixed sample of police recruits at the beginning of police training and control subjects who were comparable in age, gender, and education. Hashemi et al. therefore identified a defensive freezing behaviour as a promising somatic marker for vulnerability to stress and anxiety [Has21].

Aigrain et al. conducted a study on automatic stress detection based on micro (e.g. FACS) and macro (e.g. quantity of movement, or posture change) features with a timed arithmetic task. They extracted features from a Microsoft Kinect depth camera. With the help of a support vector machine (SVM), they were able to detect stress with 77% accuracy [Aig15]. One study explicitly explored the stress reaction following the TSST with a multimodal approach. Their results showed an increase in voice pitch (mean, minimum and variation in fundamental frequency), a decreased skin temperature, and reduced hand movements during psychosocial stress, with striking similarities between men and women [Pis18].

In a previous study using a protocol similar to this thesis, Richer et al. were able to classify individuals in a stressed condition from a stress-less control condition using MoCap data with an accuracy of 80%. The small sample size (18 participants) and a very unbalanced ratio of female to male participants may limit a good generalization of the results [Ric22].

Gait & Inflammation

Dynamic movements, such as walking, could provide even more information about changes in movement patterns that would not be observed in static poses. Gait analysis has proven useful in many clinical applications to diagnose and monitor certain diseases [Jar18].

Some brain diseases, such as attention deficit hyperactivity disorder, autism, dementia, Parkinson's disease, depression, Pick's disease, or bipolar disorder, slow down body movement as well as hand and foot movements [Jar18].

In this context, the results of Lasselin et al. are of great importance. In their work, they induced systemic inflammation (which are also triggered by acute stress [Roh19]) by an intravenous injection of lipopolysaccharide, followed by TUG and walking tests. During inflammation compared to placebo, participants showed shorter, slower and wider strides, less arm and knee extension as well as an downward tilted head. These results show that motion clearly contains information about the inflammatory status of an individual, which could be used in future work to automatically recognize if someone is sick [Las20].

Another promising approach for the non-invasive detection of inflammation are facial cues. A paper by Axelsson et al. used a similar approach to Lasselin et al. [Las20] by inducing inflammation with lipopolysaccharide, but focused on facial features rather than body movement. Acutely ill patients were judged by observers to have paler lips and skin, a puffier face, drooping corners of the mouth, reddened eyes, less shiny skin, and to be more tired [Axe18].

Gender Differences

The influence of gender on the perception and expression of affective states is largely unexplored. Most of the studies focus rather on gender differences in perception of emotions than the differences in expression, with the main focus on facial expressions. Previous research showed that there are diverse and sometimes conflicting findings about the abilities of men and women to decode facial expressions [Kar13].

In a study by Camurri et al., participants tended to apply social stereotypes to infer the gender of a PLD throwing a ball with different emotions. Angry movements were shown more frequently by men, while sad movements were more attributed to women [Cam04]. Similarly, the perception of anxious gait is facilitated for females, which may be due to kinematic similarities between anxious gait and natural female gait [Kap05].

The sometimes contradictory results highlight the important role that gender may play in the perception and demonstration of affective movements and underscore the importance of accounting for gender differences. For the analysis of affective-expressive movements, databases should contain a balanced number of male and female subjects to eliminate (or control for) the potential role of gender [Kar13]. Therefore, the evaluation of gender differences is also covered in this work.

Chapter 3

Methods

3.1 Data Acquisition

To assess the influence of stress on dynamic movements a study was cunducted at the *Machine Learning and Data Analytics Lab* from March to May 2022. Similar to a previous study, an intra-subject study design was used [Ric22]. Participants were asked to perform the TSST and f-TSST on two consecutive days, respectively. The order of the conditions was changed weekly to obtain a balanced data set with regard to the condition order.

3.1.1 Study Population

In total, 41 participants (18 female and 23 male) have been recruited for the study. An overview of gender and condition order for all participants can be found in Table 3.1, demographic and anthropometric data of the participants is shown in Table 3.2.

Table 3.1: Gender and condition order overview

Condition order	Gender		Total
	Female	**Male**	
f-TSST first	10	12	22
TSST first	8	11	19
Total	18	23	41

Participants were recruited using electronic flyers, which were distributed via social media and with mail distribution lists. To check their eligibility for the study, participants were asked to fill out a screening questionnaire prior to the study. Exclusion criteria included an age below 18 or above 50 years, non-German native language, a BMI lower than 18 or higher than 30, physical or mental illnesses of any kind, intake of medication, smoking, drug use,

Table 3.2: Demographic and anthropometric data of the participants; Mean ± SD

	Age [years]	**Height** [cm]	**Weight** [kg]	**BMI** [kg/m^2]
Female	24.06 ± 2.69	173.00 ± 10.41	65.81 ± 9.98	21.91 ± 1.93
Male	24.04 ± 4.14	177.87 ± 10.27	70.48 ± 10.80	22.20 ± 2.14
All	24.05 ± 3.54	175.73 ± 10.50	68.43 ± 10.58	22.07 ± 2.03

adiposity, and former participation in a similar stress test. As compensation for participation in the study, participants had the option to either receive 50 € or 5 *Versuchspersonenstunden* (for psychology students).

3.1.2 Acute Stress Induction

For stress induction, the TSST was used, which is the gold standard for assessing acute psychosocial stress in a laboratory setting [Dic04]. The f-TSST was used as a control condition, which should not activate the HPA axis or increase the negative affect [Wie13]. An overview of the differences between the f-TSST and TSST protocols can be found in Figure 3.1.

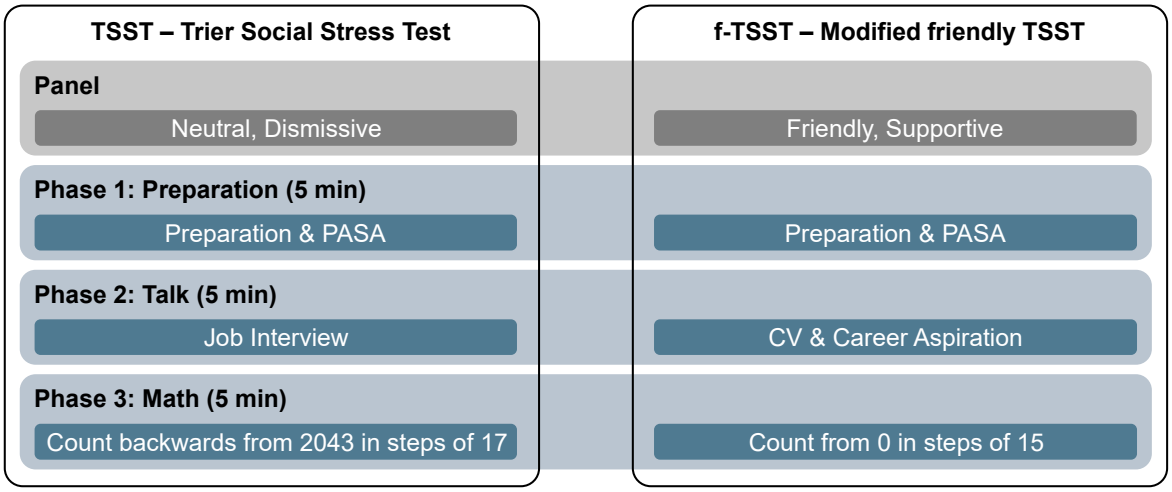

Figure 3.1: Protocol comparison of TSST and f-TSST

TSST

The TSST was performed in front of a two person panel consisting of one female and one male experimenter wearing white lab coats. The panel was instructed to be completely neutral and show as little as possible reaction to the participants actions. The active part of the panel was always the opposite gender to the participant and seated on the right side from the participants perspective.

The protocol consisted of three 5 minute phases: Preparation, talk, and math. After the study leader had explained the task and left the room, the preparation phase began. The explanation of the task included that participants should imagine that the panel is responsible for deciding if the participants should get their dream job. Additionally, it was explained that the professional qualifications are already known, therefore participants should tell the panel something about their personality. Participants were given three minutes to take notes for the upcoming interview-style conversation and two minutes to complete the primary appraisal secondary appraisal (PASA) questionnaire [Gaa09]. The PASA is well-established measure designed to assess cognitive appraisal processes in a stressful situation [Car16].

Once the preparation phase was complete, two cameras (for details about the cameras see Section 3.1.4) were turned on and participants were instructed to begin their interview. Participants were expected to speak as long as possible without interruption. The panel intervened only when participants did not talk about their personality or when participants remained silent for more than 20 seconds. Then, in the final phase, participants were asked to perform a mental arithmetic task, where they were asked to count backwards from 2043 in steps of 17. Anytime a mistake occurred, the panel intervened and the participant was instructed to restart at 2043.

f-TSST

Similar to the TSST, the f-TSST was performed in front of a two person panel. However, the f-TSST was designed to induce as little stress as possible while maintaining a setting comparable to the TSST. Thus, the panel did not wear lab coats and was instructed to be friendly and supportive throughout the whole protocol. Additionally, the panel member of the opposite gender to the participant left the room during the preparatory phase.

The talk part of the f-TSST is designed to be rather a conversation about the CV and career aspiration of the participant, than a stressful job interview. Since the original f-TSST protocol does not include any math part, the math part of the placebo-TSST [Het09], another proposed stress-less control condition of the TSST, was used. During this math part, participants were asked to count in steps of 15 starting at 0. If a mistake was made, they were made aware of the mistake in a friendly way and asked to continue from the last correct number.

3.1.3 Gait & Mobility Tests

For each day, a total of four gait and mobility tests were performed at fixed times relative to the intervention, as shown in Table 3.3. These time points were chosen to match the following events: Baseline (as little stress load as possible), directly after the TSST or f-TSST ((f-)TSST) (to assess to impact of acute threat), 20 min after the (f-)TSST (at the expected cortisol peak),

and as late as possible (to assess the influence of inflammation). The TUG and 4×10 m gait tests were chosen according to previous work that assessed the influence of inner state changes, specifically inflammation, on human motion, e.g. [Las20].

TUG

The TUG [Pod91] is a standard clinical procedure for assessing the functional mobility. The test is performed by taking the time the participant needs to rise from a chair, walk 3 meters, turn, walk back, and sit down again, as schematically shown in Figure 3.2.

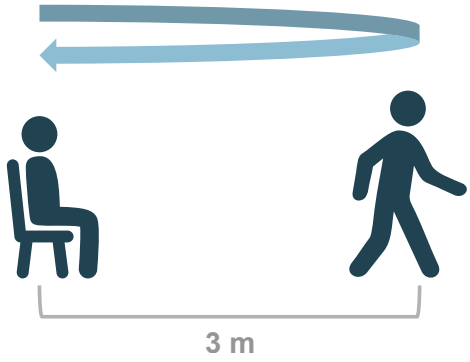

Figure 3.2: TUG schematic procedure

Gait Tests

For assessing changes in gait, we used the 4×10 m gait test, where participants are asked to walk a distance of 10 m back and forth twice, as sketched in Figure 3.3. This kind of test was already successfully used in the context of Parkinson's disease [Bar11].

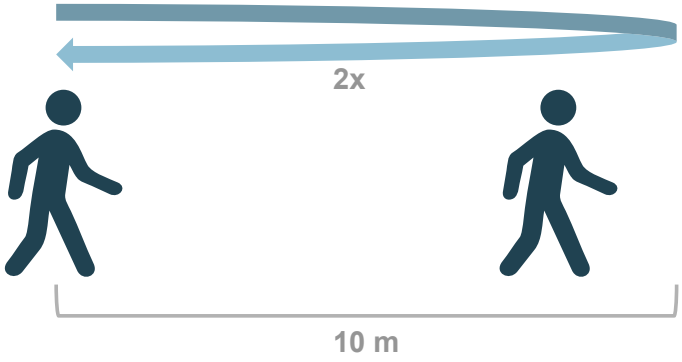

Figure 3.3: 4×10 m gait test schematic procedure

3.1.4 Procedure

Pre-Test Phase

After arriving at the laboratory, participants were guided to the preparation room, seated, and asked to sign a declaration of consent. Next, the study leader roughly explained the timeline of the study. After taking the first saliva sample (S_0), the first dried blood spot (DBS) sample was obtained (B_0). From DBS samples the inflammatory marker c-reactive protein (CRP) can be extracted. An overview of the sampling times of saliva, DBS, and gait & mobility tests can be found in Table 3.3.

Table 3.3: Sampling times relative to (f-)TSST start

Relative time [min]	-40	-1	0-15	$+16$	$+25$	$+35$	$+45$	$+60$	$+75$
Saliva samples	S_0	S_1		S_2	S_3	S_4	S_5	S_6	S_7
DBS samples	B_0		*(f-)TSST*						B_1
Gait & mobility tests	G_0				G_1	G_2			G_3

After S_0, participants were provided with 200 ml of grape juice (or 200 ml of sugar water for fructose intolerant participants), to minimize effects due to interindividual differences in energy availability as shown in previous studies [Zän20]. On the second day, female participants gave a passive drool sample, to determine progesteron levels to detect menstrual cycle-related changes of the cortisol response to acute stress [Ham20].

Body weight, body fat percentage, and muscle percentage were determined using a body scale. Diverse measurements, e.g. body height, shoulder height, shoulder width, required for the use of the Xsens MVN Awinda MoCap system were taken. The Xsens MVN Awinda MoCap (Xsens, Enschede, Netherlands) is an inertial measurement unit (IMU)-based system consisting of 17 sensor node, attached to the body with velcro straps. ECG data were recorded using a wearable ECG sensor node (Portabiles GmbH, Erlangen, Germany), attached to a chest strap, recording a 1-channel ECG according to Lead I of Einthoven's Triangle with a sampling frequency of 256 Hz. Additionally, hip and waist circumference were measured. Subsequentially, participants completed several self-report questionnaires, which will be explained in detail in Section 3.1.5.

Before each MoCap recording, a short calibration routine (*N-pose & Movement* as defined by Xsens MVN [Xse21]) was performed.The first trial of gait & mobility tests (G_0) consisted of one iteration of the TUG and two iterations of the 4×10 m gait tests. A separate recording was obtained for each of trial of the gait and mobility tests and during the (f-)TSST. Participants were asked to walk at their preferred speed. Afterwards, the cadence during baseline, defined as the number of steps per time period, was computed by dividing the total number of steps by the elapsed time, measured by a stop watch.

(f-)TSST

Circa 40 min after arrival the participants were brought to a second room where the (f-)TSST was conducted as described in Section 3.1.2. MoCap data were recorded during the whole protocol. In addition, two cameras recorded the talk and math phase of the (f-)TSST: One RGB camera (Sony SRG-300H, Minato, Japan) was filming the face, a RGB-D camera (Microsoft Azure Kinect, Redmond, WA) was filming the entire body. The panel used a smartphone application to log the phases of the (f-)TSST for later extraction of the MoCap and video data.

Post-Test Phase

After finishing the (f-)TSST, participants were brought back to the preparation room, where the next saliva sample (S_2; 15 min relative to (f-)TSST start) was obtained. Then, they were asked to complete the next set of self-report questionnaires, including positive and negative affect schedule (PANAS) [Wat88]. An overview of all questionnaires can be found in Table 3.5.

The following two saliva samples (S_3 and S_4) were obtained at 25 min and 35 min, respectively. Each saliva sample was followed by one trial of the gait & mobility tests (G_1 and G_2). Participants were asked again to perform the TUG and two iterations of the 4×10 m gait tests. In contrast to the baseline measurement G_0, only one of the 4×10 m walks was performed at preferred speed, for the second iteration participants were instructed to match their walking speed to a metronome played from a smartphone. The speed of the metronome was configured to match the participants gait cadence from the baseline trial of the first day of the study. Cadence matching was performed to expose alterations in walking motions that are cadence dependent.

Afterwards, participants were asked to fill out an ethics to assess attitude patterns towards the use of AI-based sensor technology (Day 1 only). The evaluation of this questionnaire is not covered in this thesis.

The next saliva samples were taken at 40 min (S_5), 60 min (S_6), and 75 min (S_7), respectively. Right after the last saliva sample another DBS sample (B_1) was collected, and another trial of the gait & mobility tests was performed (G_3).

At the end of a session participants were either reminded about their next session on the following day (Day 1) or debriefed and asked to sign a non-disclosure agreement regarding the setup of the study (Day 2).

3.1.5 Measurements

Motion Capture Data

MoCap data were recorded with Xsens MVN software at a sampling rate of 60 Hz and saved as .mvn files. The recordings were then manually trimmed to only include one iteration of the TUG or the 4×10 m gait tests and exported to MVN open XML format (.mvnx). .mvnx files include frame-wise information about all 23 body segments and 22 joints, as well as data of 17 IMU sensors, center of mass, and foot contacts. An overview of the recorded channels can be found in Table B.1. Definition of the segments are shown in Figure 3.4.Additionally, several body parts were aggregated to groups reflecting movements of one specific body area (Table 3.4 and Figure 3.4).

Table 3.4: Body part group definitions. {L/R}: Left and right side.

Group	Body Parts
Trunk	Pelvis, L3, L5, T8, T12, Neck
Upper Extremities	{L/R} Shoulder, {L/R} Upper Arm, {L/R} Fore Arm, {L/R} Hand
Lower Extremities	{L/R} Upper Leg, {L/R} Lower Leg, {L/R} Foot, {L/R} Toe
Total Body	All body parts

Endocrinological Data

During the procedure, a total of eight saliva samples were collected per session to assess cortisol as a measure for HPA axis reactivity to acute psychosocial stress. Two saliva samples were taken before the start of (f-)TSST and six afterwards, as listed in Table 3.3. The saliva samples were collected with Salivettes (Sarstedt AG & Co. KG, Numbrecht, Germany) as described in previous studies [Ric21a]. The samples were kept at room temperature until the end of the session and were then stored in a freezer at a temperature of −18 °C until the end of the study. In the laboratory, the cortisol concentrations were extracted from the saliva samples as described in previous work [Ric21a].

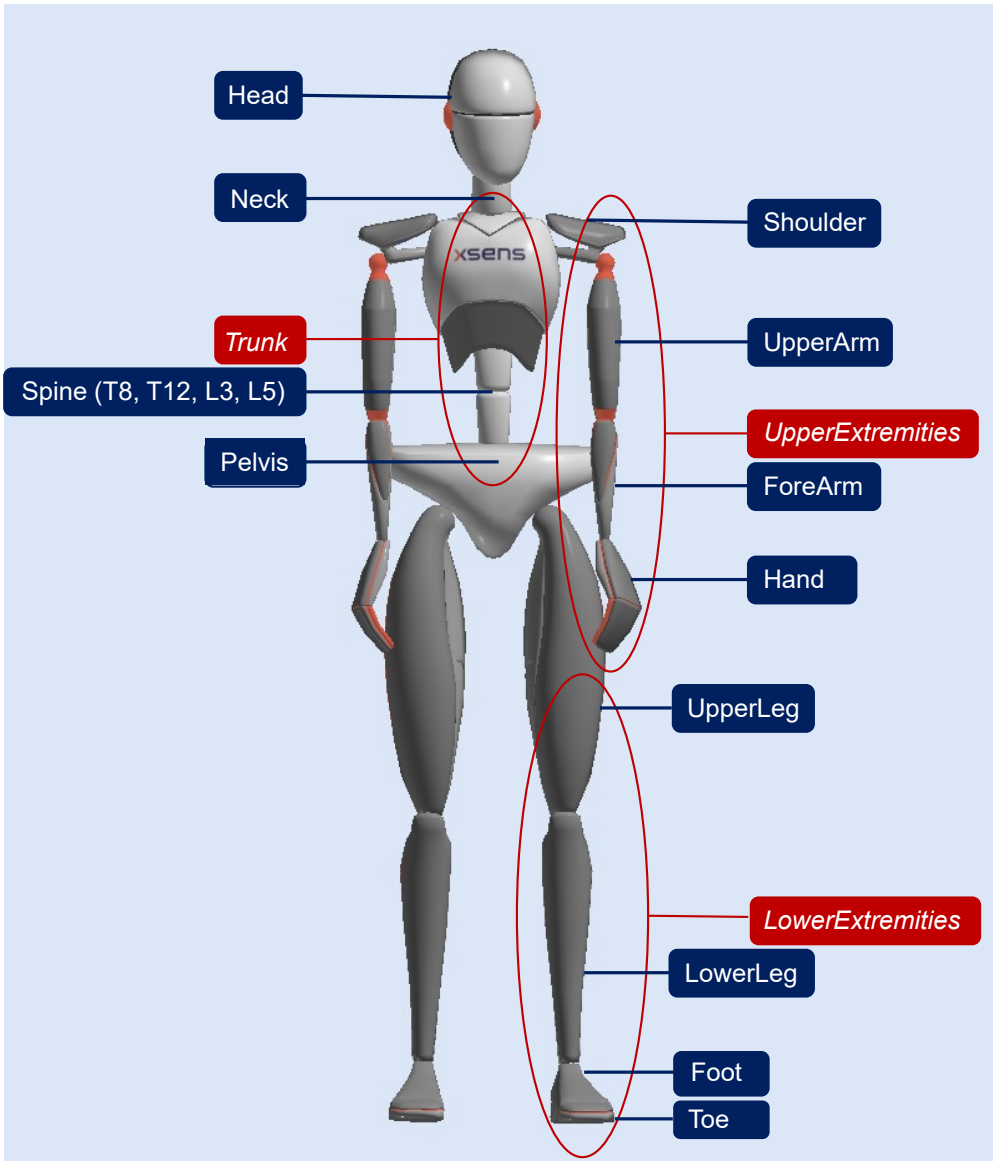

Figure 3.4: Xsens body part definition. Body parts are labeled in blue, body part groups are labeled in red.

Self-Report Data

During the course of the study, participants were asked to complete several psychological questionnaires. The first set of questionnaires was provided in the screening phase, after participants were found to be eligible for study participation as described in Section 3.1.1. The second set of questionnaires was completed on each of the two study days before the intervention ((f-)TSST). The third set was completed on both study days right after the (f-)TSST. On overview of all questionnaires can be found in Table 3.5. For this work, only PASA, PANAS, and state-trait anxiety-depression inventory (STADI) trait will be evaluated.

Table 3.5: Overview of all questionnaires

Set	Screening	Pre	Post
Questionnaires	ADS-L	STADI State	STADI State
	STADI Trait	PANAS	PANAS
	Brief-Cope	SSSQ	SSSQ
	PSS		VAS
	BFIK		SSSGS
	RSE		
	SCS-D		
	RSQ		
	BES		
	SOC		
	TSGS		

3.2 Stress Response Assessment

3.2.1 Endocrinological Measures

The cortisol response, which is reflecting HPA axis activity, was assessed using the samples S_1-S_7. From the raw cortisol values, four parameters were derived: maximum cortisol increase (Δc_{max}), area under the curve with respect to ground (AUC_g), area under the curve with respect to increase (AUC_i), and slope from S_1 to S_4 (m_{S1S4}) according to Pruessner et al. [Pru03].

The maximum cortisol increase (Δc_{max}) was computed as the difference between the maximum cortisol level after the (f-)TSST and the cortisol level before the (f-)TSST (Equation 3.1).

$$\Delta c_{max} = max(S_i) - S_1, \quad \forall i \in [2, 7] \tag{3.1}$$

The area under the curve was computed to assess the total amount of released cortisol as response to the (f-)TSST. AUC_g is computed according to Equation 3.2 using the trapezoidal rule, where S_i is the cortisol value at time point t_i and Δt_i is the time difference between two consecutive samples S_i and S_{i+1} in minutes.

$$AUC_g = \sum_{i=1}^{6} \frac{(S_{i+1} + S_i) \cdot \Delta t_i}{2} \tag{3.2}$$

Additionally, the area under the curve with respect to increase (AUC_i) was computed, which is defined as:

$$AUC_i = (\sum_{i=1}^{6} \frac{(S_{i+1} + S_i) \cdot \Delta t_i}{2}) - (6 \cdot S_1) \tag{3.3}$$

The slope between S1 and S4 (m_{S1S4}) is calculated as:

$$m_{S1S4} = \frac{S_4 - S_1}{t_4 - t_1} \tag{3.4}$$

3.2.2 Self-Report Measures

From the questionnaire scores, the differences between pre- and post-(f-)TSST were computed to assess (f-)TSST-induced changes in the state variables. For the PANAS, two scores were evaluated: PANAS positive affect (PANAS-PositiveAffect) and PANAS negative affect (PANAS-NegativeAffect). For the PASA questionnaire, PASA-Threat and PASA-Challenge scores were computed. Because the PASA questionnaire was completed during (f-)TSST, after the preparation and before the actual talk phase, the scores serve as a measure for perceived threat and challenge during the (f-)TSST [Gaa09].

3.3 Body Posture & Movement Feature Calculation

3.3.1 (f-)TSST Features

This subsection describes the feature calculation performed on the MoCap data recorded during the stress and control intervention. Most of the features used in this section are similar to previous work by Richer et al. [Ric22], and can be divided into two categories: generic and expert features.

Generic features require no previous domain knowledge and include basic statistical measures like mean, standard deviation, or coefficient of variation, as well as signal characteristics such as entropy, or energy of the signal. *Expert features*, on the other hand, assume prior knowledge and are explicitly designed to characterize movement patterns reported by previous work, or observed during data collection. Examples would be the distance of the hands or the detection of static periods. An overview of the calculated generic features can be found in Table 3.6, expert features are listed in Table 3.7. Generic features were calculated for the body parts head, total body, upper extremities, lower extremities, trunk, chest, right and left hand (Channels: vel, acc, gyr), as well as for the elbow, knee and head joint angles, and the center of mass.

Table 3.6: Generic features overview

Name	Short Form
Mean	mean
Coefficient of variation	cov
Maximum value	max_val
Absolute maximum	abs_max
Entropy	entropy
Mean crossings	mean_crossings
Zero crossings	zero_crossings
Absolute energy	abs_energy
Fast fourier transform (FFT) mean	fft_mean
FFT variance	fft_variance
FFT skew	fft_skew
FFT kurtosis	fft_kurtosis

Table 3.7: Expert features overview

Name	**Short Form**	**Channels**	**Metrics**
Static Periods	stat_periods	gyr, vel	count_per_min max_duration mean_duration sd_duration ratio
Below Threshold	below_thres	gyr	count_per_min max_duration mean_duration sd_duration ratio
Euclidean Distance	eucl_dist	pos	mean count_per_min max_duration mean_duration sd_duration ratio

Static Periods (stat_periods)

To quantify the expected freezing behavior, *static periods* were calculated over windows of 0.5 s with an overlap of 50%. A window was defined as static if the total variance in this window was below $1{\times}10^4$ (m/s)^2 for the norm of the velocity, or below $5\,(\mathrm{deg/s})^2$ for the angular velocity norm. These thresholds were determined by using test data. Based on assumptions from previous work [Ric22], this feature was calculated for the followings body parts or body part groups: Head, Chest, Trunk, Hands, Upper Extremities, and Lower Extremities. For body part groups a static periods was detected when all of the boy parts were static at the same time.

Table 3.8: Expert feature metrics

Metric	Definition
count_per_min	Number of occurences per min
max_duration	Longest duration
mean_duration	Mean duration
sd_duration	SD duration
ratio	Ratio of total time

Below Threshold (below_thres)

Below threshold is a measure on how many samples are below certain threshold. According to previous work [Ric22], this threshold was defined as a ratio of the maximum signal value. This is an additional measure to quantify the expected freezing behavior during acute stress. The ratio was set to 10%, resulting in the definition in Equation 3.5. The ratio was determined by using test data. Below threshold was calculated for Head, Chest, Trunk, Hands, Upper Extremities, and Lower Extremities.

$$\mathrm{below\_threshold}(x) = \begin{cases} True, & \text{if } ||x||_2 < 0.1 \cdot max(x) \\ False, & \text{otherwise} \end{cases} \tag{3.5}$$

Euclidean Distance (eucl_dist)

Observation revealed that participants who are under acute stress place their hands closer together, touched their heads more frequently, and adopted a more tense posture. Therefore, *euclidean distance* was calculated between Left Hand & Right Hand, Hands & Head, and Left Foot & Right Foot. Additionally to the mean distance over one period, contacts between the two body parts were determined by applying a threshold on the euclidean distance data. This threshold was set to 20 cm for hand to hand and to 25 cm for hand to head and foot to foot. The thresholds were determined based on previous experiments.

3.3.2 Gait & Mobility Tests

TUG

In clinical use, the only evaluated feature of the TUG is the TUG completion time [Pod91]. To gain better insight, additional features were calculated based on previous work by Lasselin et al. [Las20].

TUG completion time (or TUG time) was defined as the time between the beginning of the motion of the chest segment to the end of the motion of the same segment. Motion was defined as the velocity norm across all three axes higher than 0.05 m s^{-1} ($||vel_{chest}||_2 > 0.05$), as previously determined by experiments. For an example, see Figure 3.5.

First step length was calculated based on the stride detection of Zeni et al. [Zen08]. The distance between the foot at the start and the foot after two strides was calculated for each side. The first step length was defined as the maximum between left and right, since the foot that traveled the longer distance is in front at the end of the second stride and is therefore the reference for the step length.

Time to stand up was calculated between the start of the motion, as previously defined, and the first time that the left or right upper leg was vertical, where 0° is vertical. Additionally, minimum and maximum *head angle* and *chest angle* were calculated.

Table 3.9: TUG parameters overview

Temporal Parameters	Unit	**Spatial Parameters**	Unit
TUG completion time	s	first step length	m
time to stand up	s	min/max head angle	°
		min/max chest angle	°
		number of steps	-

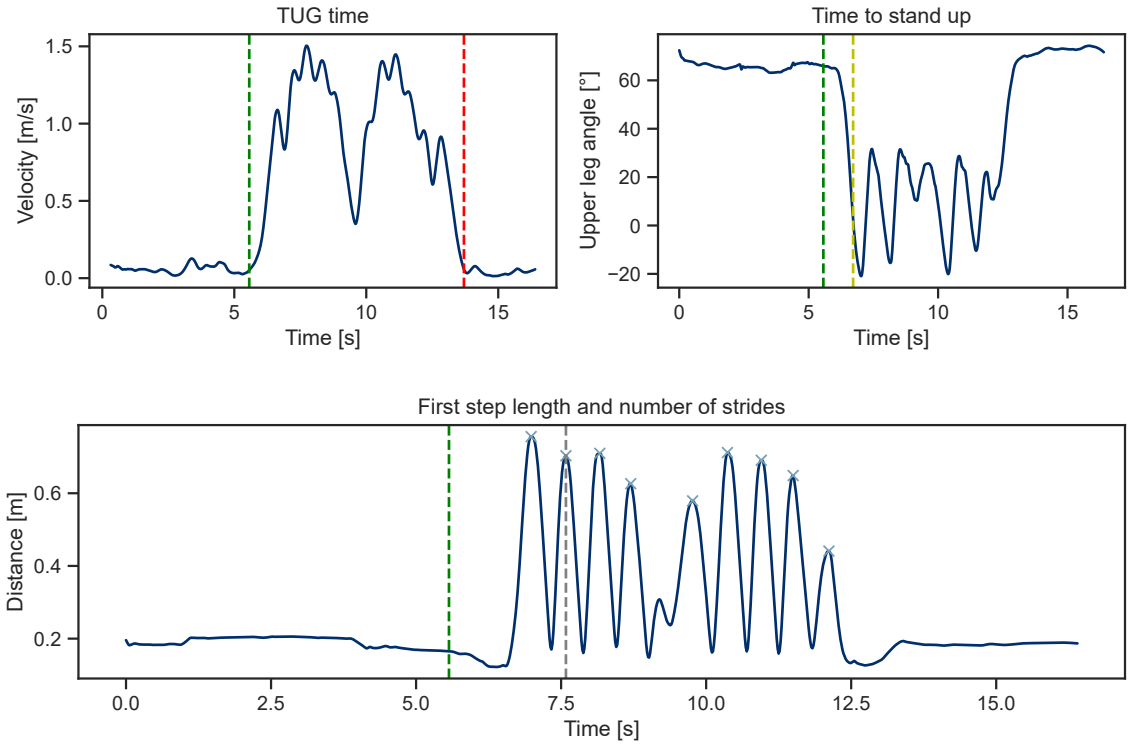

Figure 3.5: TUG features example; green: TUG start, red: TUG end, yellow: end of time to stand up, grey: end of first step, blue crosses: strides

Gait Tests

Similar to the features from the stress task, the parameters extracted from the gait tests can be divided into generic features and expert features, which are commonly referred to as spatio-temporal features in gait analysis.

Spatio-Temporal Features

For evaluating the 4×10 m gait tests, a stride detection resembling the method of Zeni et al. was used [Zen08]. The schematic gait cycle with important stride events is shown in Figure 3.6. The maximum displacement of the foot for the initial contact (IC) was calculated by taking the maximum of the euclidean distance between the pelvis and the center of the foot. For the terminal contact (TC) the toe segment was used. The mid stance (MS) definition was adapted from Rampp et al., where the MS is defined as the minimum energy of the angular velocity over all axes [Ram15].

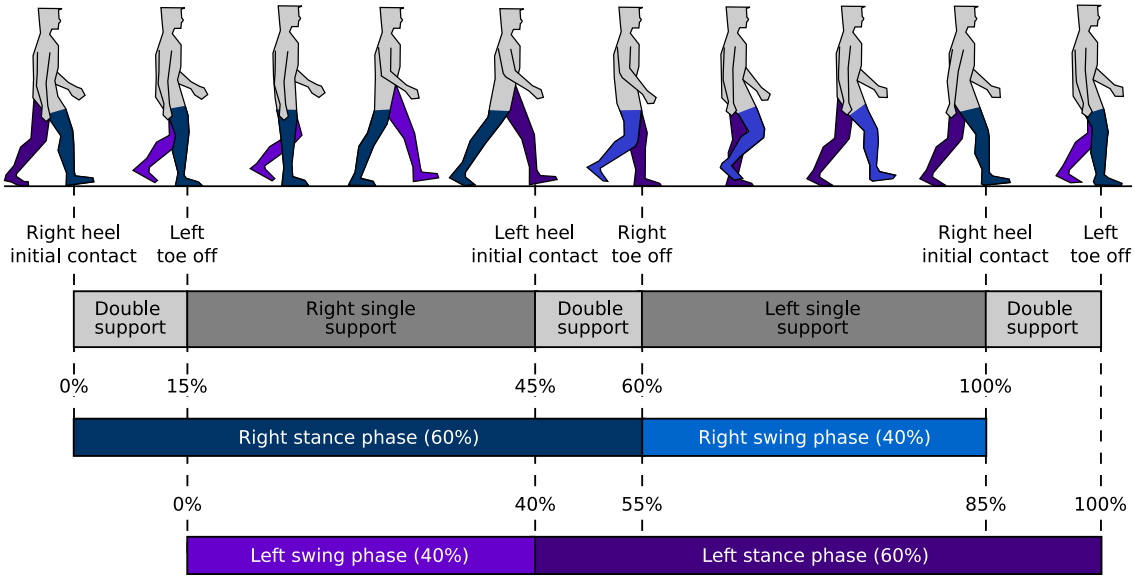

Figure 3.6: Schematic gait cycle; © Nils Roth, 2022, reprinted with permission

Turning strides were omitted, as they differ largely from strides during a continuous straight walk. To identify turning strides, the hip angle in the horizontal plane was calculated. Then, the difference between the angle of the hip before and after a stride was computed. If that difference exceeded 5°, the stride was identified as a turning stride and therefore excluded from further evaluations.

After calculating and cleaning these stride events, spatio-temporal gait parameters were extracted. For the temporal parameters stride time, swing time, and stance time were calculated. The spatial parameters were calculated based on Rampp et al. and Kanzler et al. [Ram15; Kan15]. Spatial parameters included stride length, gait velocity, and arc length. Additionally, based on previous work by Lasselin et al. [Las20], maximum and minimum knee and arm flexion angles were computed per stride. All calculated parameters can be found in Table 3.10.

Table 3.10: Spatio-temporal gait parameter overview

Temporal Parameters	Unit	**Spatial Parameters**	Unit		Unit
stride time	s	stride length	m	knee flexion	°
stance time	s	gait velocity	$m\,s^{-1}$	arm flexion	°
swing time	s	arc length	m	IC angle	°
		max sensor lift	m	TC angle	°
		max lateral excursion	m	turning angle	°

3.4 Evaluation

3.4.1 Statistics

Due to a sample size larger than 30 the distribution of the samples can be considered normal, according to the central limit theorem [Kwa17]. Therefore, for the statistical evaluation a repeated measures analysis of variance (ANOVA) could be used as statistical test with paired t-test as post-hoc test. These tests were selected based on the within-subjects design, in which the control and intervention samples are interdependent because all participants were exposed to both conditions. All statistical analyses were performed using the Python package *biopsykit* [Ric21b] based on *pingouin* [Val18]. t-test effect sizes were expressed as Hedge's g. No multi comparison correction was used due to the highly explorative character of the study [Gel12; Str11]. The following notation was used to indicate statistical significance in Figures and Tables: $^{*}p < 0.05$,** $p < 0.01$,*** $p < 0.001$.

3.4.2 Stepwise Backward Multiple Linear Regression

Similar to the work of Lasselin et al. [Las20], stepwise backward multiple regression (SBMLR) was performed to examine the relationship of cortisol and self-report scores to movement. Only the motion data obtained during the (f-)TSST were used. The difference from f-TSST to TSST features was calculated to quantify movement differences. Feature data were standardized by means of z-score normalization. The dimensionality of the motion features was reduced by applying principal component analysis (PCA). The number of PCA components was chosen such that the explained variance was at least 80%. Multicollinear correlated features were removed with a threshold of 0.8.

Finally, SBMLR was performed for each self-report and biomarker individually, using feature data from a single body part, or multiple body parts. For regression analyses, motion features were used as predictors, and a biomarker or self-report score was used as the dependent variable.

SBMLR is performed iteratively by running a linear regression for the predictors and removing the predictor with the highest p-value. The best fitting model is determined by selecting the regression model with the highest adjusted R^2 value.

3.4.3 Classification

ML models were trained to differenciate stress from non-stress conditions from the motion features obtained during the (f-)TSST. Classification was performed using a standard ML pipeline, as outlined in Figure 3.7.

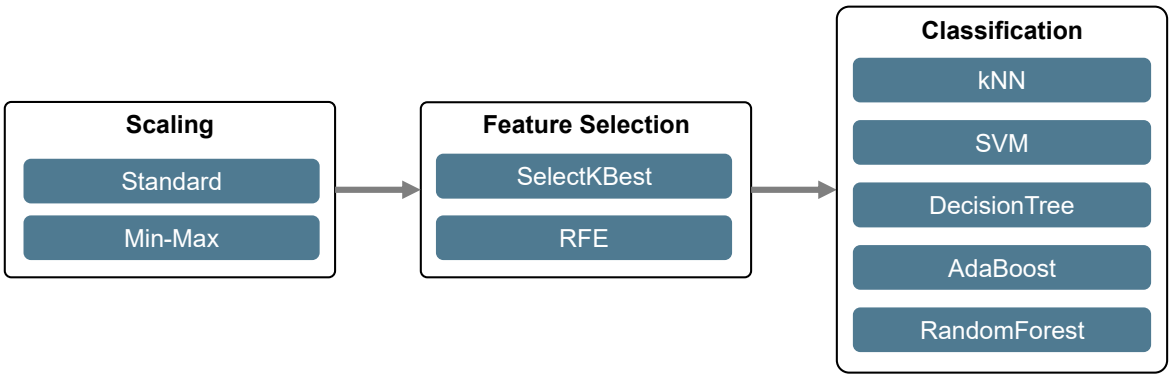

Figure 3.7: Classification pipeline

Five different models were trained for classification: k-nearest neighbors (kNN), DecisionTree, SVM, AdaBoost and RandomForest classifiers. Models were evaluated by maximum accuracy using a five-fold cross validation (CV). Within each iteration of the CV, the hyperparameters of the feature selection and the classifier were optimized using a five-fold CV with grid search (random search with 10 000 trials for RandomForest). Within each fold of the CV for hyperparameter optimization, features were first scaled using using StandardScaler or MinMaxScaler. StandardScaler uses z-score normalization to scale feature distributions to a mean of 0 and a standard deviation of 1. MinMaxScaler maps each feature to a range between 0 and 1. Next, the dimensionality of the feature space was reduced by applying SelectKBest or RFE. SelectKBest reduces the number of features by only selecting the k features with the highest ANOVA F-score. For RFE an estimator (in this case a SVM) is trained to obtain the importance of each feature. Then, the least important features are pruned from the data recursively until the desired number of features is reached. An overview of the hyperparameter space for optimizing each model is shown in Table 3.11. This CV approach has been successfully used in previous work [Abe19].

Table 3.11: Hyperparameter grid; [1] only for RBF kernel, [2] only for poly kernel, [3] RandomizedSearch was used for RandomForest

Feature Selection	**Hyperparameter**	**Values**
SelectKBest	k	2 to 30; steps of 2; all
RFE	n	2 to 20; steps of 2
Classifier/Regressor	**Hyperparameter**	**Values**
kNN	k	2 to 20; steps of 2
	weights	uniform, distance
SVM	Kernel	linear, RBF, poly
	C	$10^{-1}, 10^{0}, 10^{1}, 10^{2}, 10^{3}, 10^{4}$
	gamma [1]	$10^{-4}, 10^{-3}, 10^{-2}, 10^{-1}, 10^{0}, 10^{1}$
	degree [2]	2 to 6
DecisionTree	criterion classification	gini, entropy
	criterion regression	squared_error, friedman_mse
	depth	2 to 20; steps of 2
	min_samples_leaf	0.1 to 0.5; steps of 0.1
	min_samples_split	0.1 to 0.8; steps of 0.1
	max_features	0.1 to 0.6; steps of 0.1; log_2, all
AdaBoost	base_estimator	DecisionTree
	n_estimators	10 to 500; steps of 20
	learning_rate	0.01 to 0.1; steps of 0.01,
		0.1 to 1.6; steps of 0.1
RandomForest [3]	bootstrap	True, False
	criterion	0.1 to 0.8; steps of 0.1
	max_depth	4 to 50; steps of 2
	max_features	auto, sqrt
	min_samples_leaf	0.1 to 0.5; steps of 0.1
	min samples_split	0.1 to 0.8; steps of 0.1
	min_weight_fraction leaf	0.0 ; to 0.5 ; steps of 0.1
	max_leaf_nodes	2 to 20; steps of 2
	min_impurity_decrease	0 to 0.1; steps of 0.01
	n_estimators	10 to 500; steps of 10
	ccp_alpha	0 to 1; steps of 0.1

3.4.4 ML-Based Regression

ML-based regression was performed analogously to the classification. Instead of predicting condition labels, the continuous endocrine and self-reported measures were predicted (Δc_{max} , PASA-Challenge and -Threat). Again, a five-fold CV was used to evaluate the models (evaluation CV), and a five-fold CV was used within each fold of the evaluation CV to optimize the hyperparameters of feature-selection and the regressors by highest R^2 value. The same scaling and feature selection methods as for the classification task were applied. Five different models were fitted in their respective regression variant: $\mathrm{kNNRegressor}$, SVR, $\mathrm{DecisionTreeRegressor}$, $\mathrm{AdaBoostRegressor}$, and $\mathrm{RandomForestRegressor}$. The hyperparameter grid is listed in Table 3.11.

Chapter 4

Results & Discussion

4.1 Stress Response Assessment

This section presents the results of traditional stress markers such as questionnaires and salivary cortisol levels.

4.1.1 Endocrinological Measures

As shown in Figure 4.1, an approx. 2-fold increase in cortisol levels was noted after TSST. Mean cortisol concentrations increased from the baseline measure S_1 to the time of the expected cortisol peak (25 min after TSST start; S_3) by 121% for the TSST. For the f-TSST, from S_1 to S_3 there was only a slight increase in mean cortisol levels (7%).

All derived cortisol features showed a significant difference for the TSST in contrast to the f-TSST, the results from the statistical test can be found in Table 4.2. The largest effect sizes were found for Δc_{max} with g = 1.024 (mean increase of 4.33 nmol l^{-1}), and m_{S1S4} with g = 1.023 (mean increase of 0.12 nmol l^{-1}). All derived features are plotted in Figure 4.3.

The results for the endocrinological response are in line with previous literature, e.g. [Wie13; All14]. The cortisol concentration levels following the TSST show an approximate 2-fold increase, while the average cortisol concentration following the (f-)TSST is only marginally increased. The relatively high difference between the conditions at S_0 relative to (f-)TSST start is probably showing by chance, as there are various influences on an individual's cortisol concentration. When evaluating the cortisol response seperately for the two condition orders, it can be seen, that the mean cortisol response to the f-TSST is strongly increased if the f-TSST was conducted on the first of two study days (Δc_{max} increased from 0.76 $\pm$ 2.92 nmol l^{-1} to 1.44 $\pm$ 2.82 nmol l^{-1}; +90 %; Figure 4.2). Additionally, the average cortisol response is slightly blunted if the TSST was conducted on the second day (Δc_{max} = 5.82 $\pm$ 4.79 nmol l^{-1} vs. 4.56 $\pm$ 4.66 nmol l^{-1}; $-$23 %). A possible explanation is that the novelty of the situation

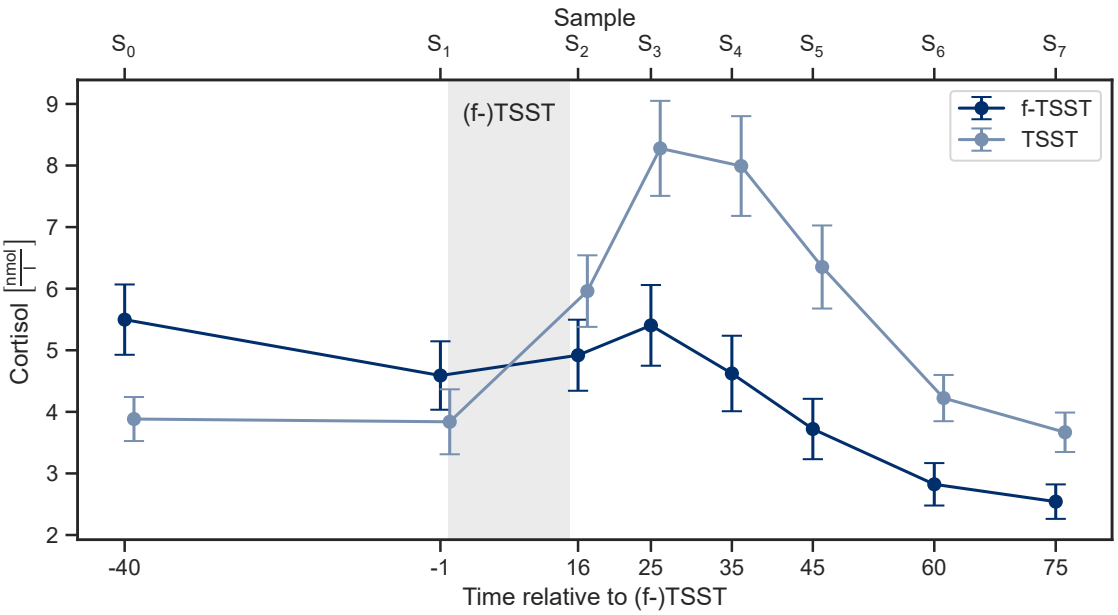

Figure 4.1: Cortisol response; Mean ± SE over all participants

is of high importance for the stress reaction of the participants. For future work, this could be a hint that a fixed condition order with TSST on the first day could be advantageous. Due to time constraints, further analyses of the saliva and DBS samples were not performed yet. Therefore, α-amylase and CRP could not be included in the evaluation. These results could provide further insights into the quality of the acute stress induction.

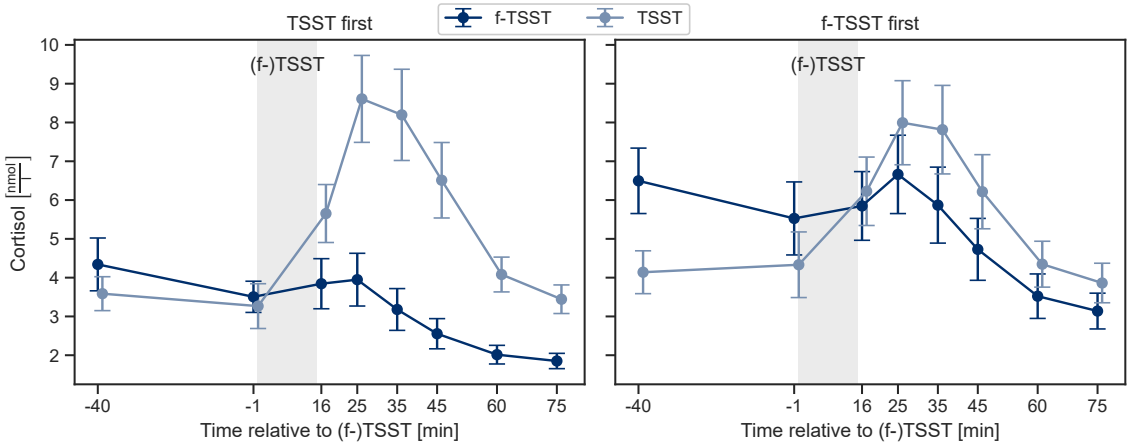

Figure 4.2: Cortisol response per condition order; Mean ± SE over all participants

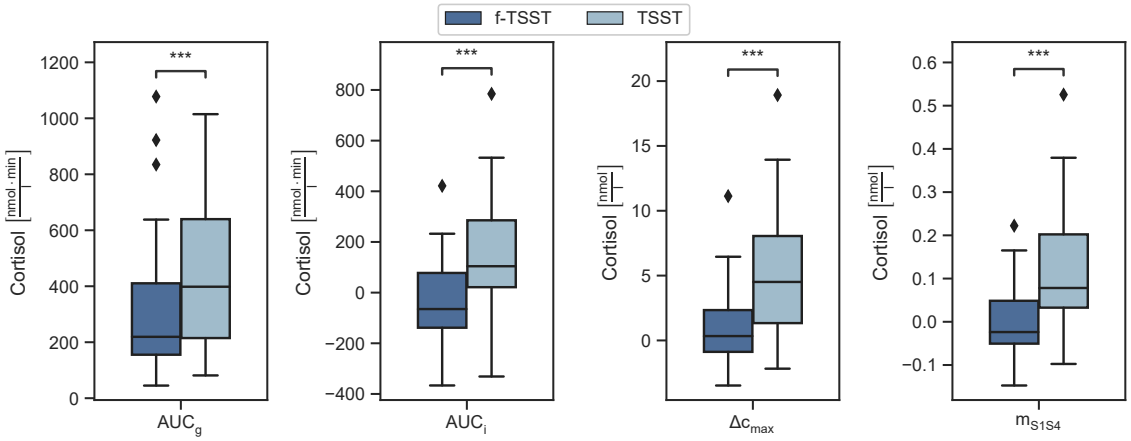

Figure 4.3: Cortisol derived features; over all participants;
$^{*}p < 0.05$, $^{**}p < 0.01$, $^{***}p < 0.001$

Table 4.1: t-test results of cortisol features; $^{*}p < 0.05$, $^{**}p < 0.01$, $^{***}p < 0.001$

Feature	$t(40)$	p	Hedges' g
AUC_g	4.223	<0.001***	0.533
AUC_i	5.509	<0.001***	0.937
Δc_{max}	5.904	<0.001***	1.024
m_{S1S4}	5.794	<0.001***	1.023

4.1.2 Self-Report Measures

All self-report measures showed a significant difference for the two conditions, as depicted in Table 3.5 and Figure 4.4 . On average, PASA-Challenge increased by 2.86 points, whereas PASA-Threat by 3.47 points. For the PANAS and the STADI subscores, the differences between pre and post (f-)TSST were evaluated. PANAS-NegativeAffect showed an average increase from -0.11 ± 0.27 for the f-TSST to 0.31 ± 0.44 for the TSST. PANAS-PositiveAffect is lower for the stress condition (-0.20 ± 0.64) compared to the control condition (0.14 ± 0.41). STADI-Anxiety was, on average, 5.29 points higher for the TSST.

These results are similar to previous studies, e.g., [Ric22; All17]. Thus, it can be concluded that the acute stress induction (TSST) as well as the control condition (f-TSST) performed in the study meet the standards in laboratory stress assessment. Further questionnaires, e.g. the short state stress questionnaire (SSSQ) were not evaluated in this work, but could provide further insights in the experience of the stressful situation of the participants.

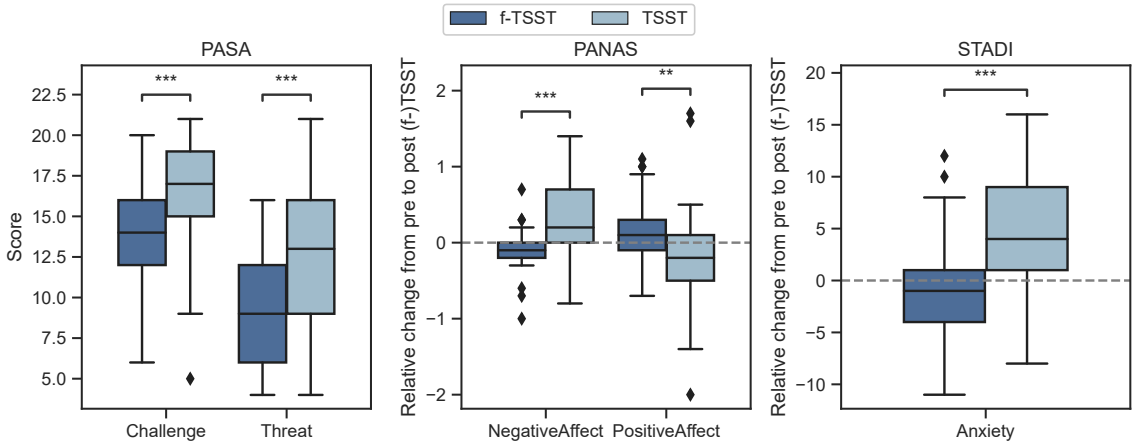

Figure 4.4: Questionnaire results; $^{*}p < 0.05$, $^{**}p < 0.01$, $^{***}p < 0.001$

Table 4.2: t-test results of self-report measures; $^{*}p < 0.05$, $^{**}p < 0.01$, $^{***}p < 0.001$

Questionnaire	Subscale	$t(40)$	p	Hedges' g
PASA	Challenge	6.351	<0.001***	0.823
	Threat	6.024	<0.001***	0.803
PANAS	NegativeAffect	6.053	<0.001***	1.138
	PositiveAffect	−2.885	0.006**	−0.635
STADI	Anxiety	4.851	<0.001***	1.040

4.2 Body Posture & Movement Feature Evaluation

Due of the large number of features, only the most relevant result will be shown in this section. The complete results of the statistical evaluation of all features can be found in Appendix A.

4.2.1 (f-)TSST Features

Two participants had to be excluded from the movement analysis during the (f-)TSST, one due to problems with the MoCap recording, one due to an uncompleted math part during TSST. Therefore, results from $n = 39$ participants are reported.

Generic Features

Figure 4.5 shows the ten generic features that showed the largest difference between the conditions (quantified by highest t-values). There are various generic features that quantify the reduced head movement during TSST compared to f-TSST, e.g. mean acceleration, or mean angular velocity norm. Additionally, the mean head flexion angle decreased for the TSST in contrast to the f-TSST ($-12.75 \pm 5.35°$ vs. $-10.60 \pm 4.21°$). The coefficient of

variation (CoV), which is defined by standard deviation (SD) divided by mean, was increased for head and left hand. The CoV is increased because the mean of the respective features decreased and the SD was on a similar level. Thus, an increased CoV, in this case, quantifies reduced movement. A lower mean angular velocity can be observed in the stress task for the chest as well as trunk. The results of the paired t-tests for all generic features can be found in Table B.2.

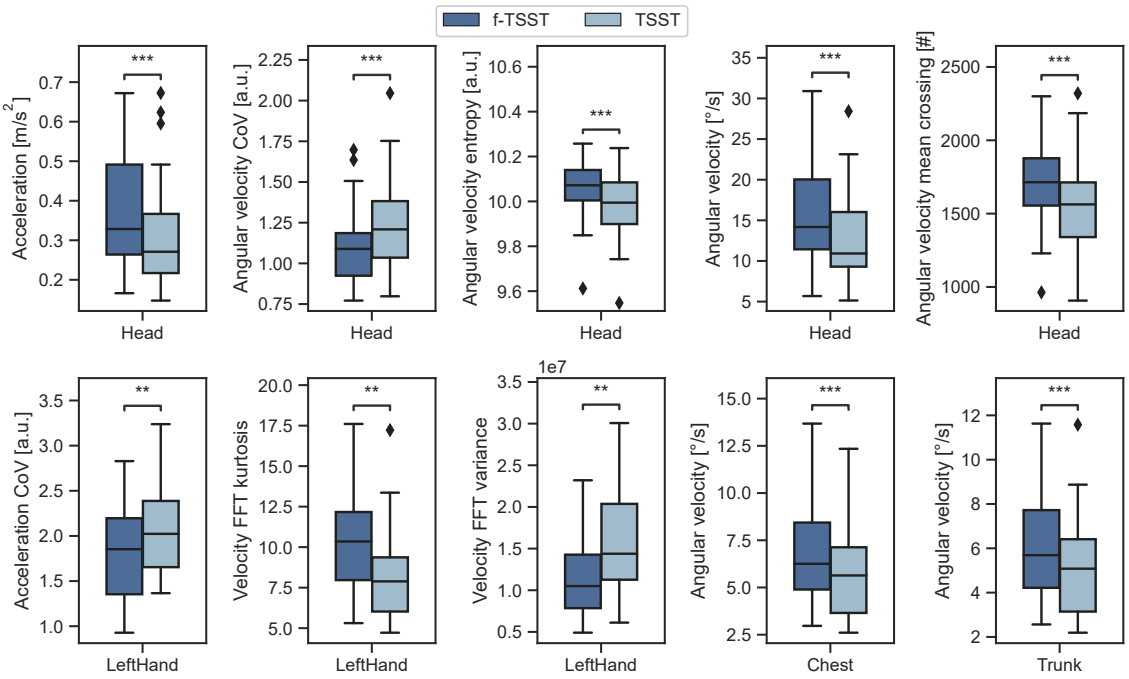

Figure 4.5: Best performing generic features (highest absolute t-value)

Expert Features

There was no statistically significant difference between the two conditions for any of the *euclidean distance* measures (Table B.3).

Static periods showed a significant difference for most of the evaluated body parts. The static periods observed during the TSST had a longer mean and maximum duration, as well as an increased static period ratio relative to the total recording time. Examples for the static periods feature for the body parts head, upper extremities, chest and total body are shown in Figures 4.6, A.3, A.4 and A.5, the full results of the statistical evaluation are shown in Table B.4. Metrics of *below threshold* showed a significant difference for head and upper extremities. For the head, the count of samples below threshold per minute as well as ratio showed an increase during the TSST. Maximum duration and ratio were increased during the TSST for upper extremities (Figures 4.7 and A.6; Table B.5).

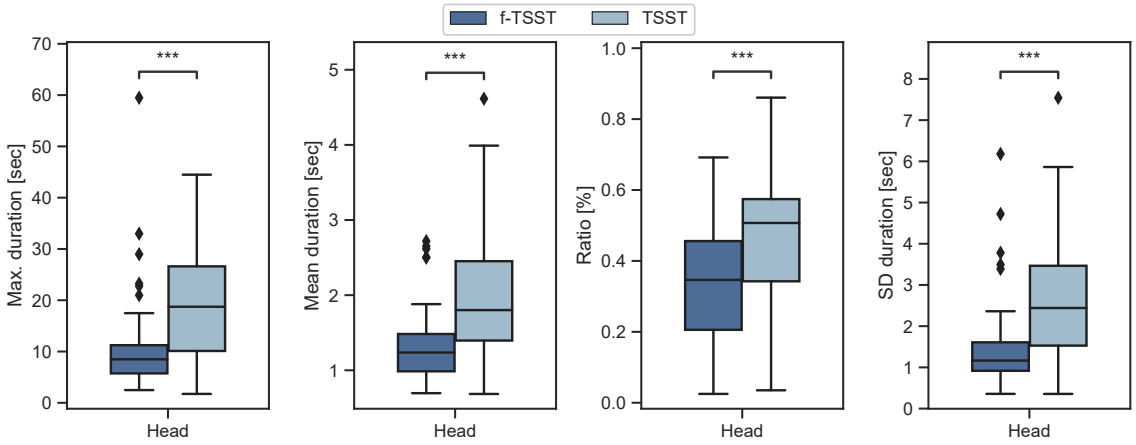

Figure 4.6: Head *static periods* feature (gyr channel)

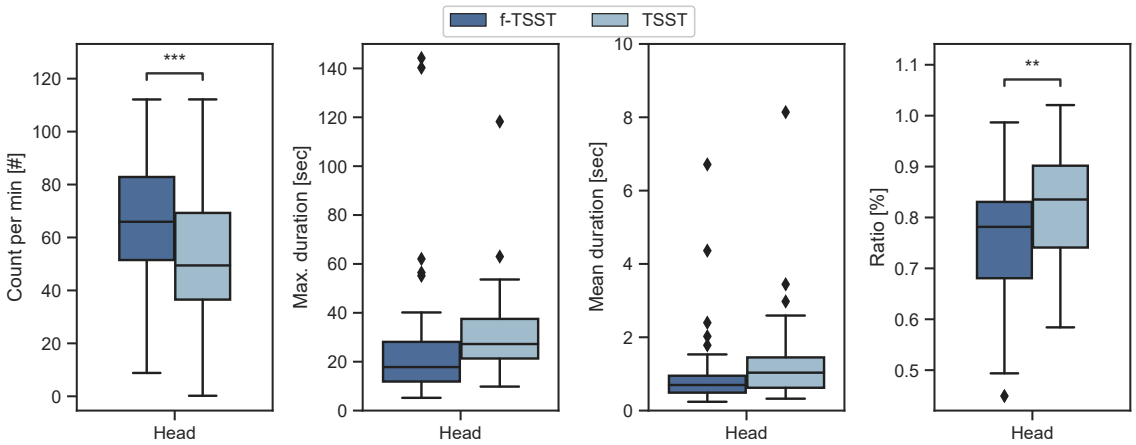

Figure 4.7: Head *below threshold* feature (gyr channel)

Gender Differences

When testing for gender differences, only few features were significantly different. Among the features with statistical differences are the mean euclidean distance between hands and head. These differences likely origin from a smaller average body height of female participants compared to male participants (Table 3.2). Since no normalization of distance features to the participants' body heights were performed, this probably leads to smaller average hand-to-head differences for female participants. Because of the similarity of the motion features, a possible conclusion could be that there is only minor differences in the bodily motion of females and males in an acute stress situation. t-test results can be found in Table B.6.

Phases of (f-)TSST

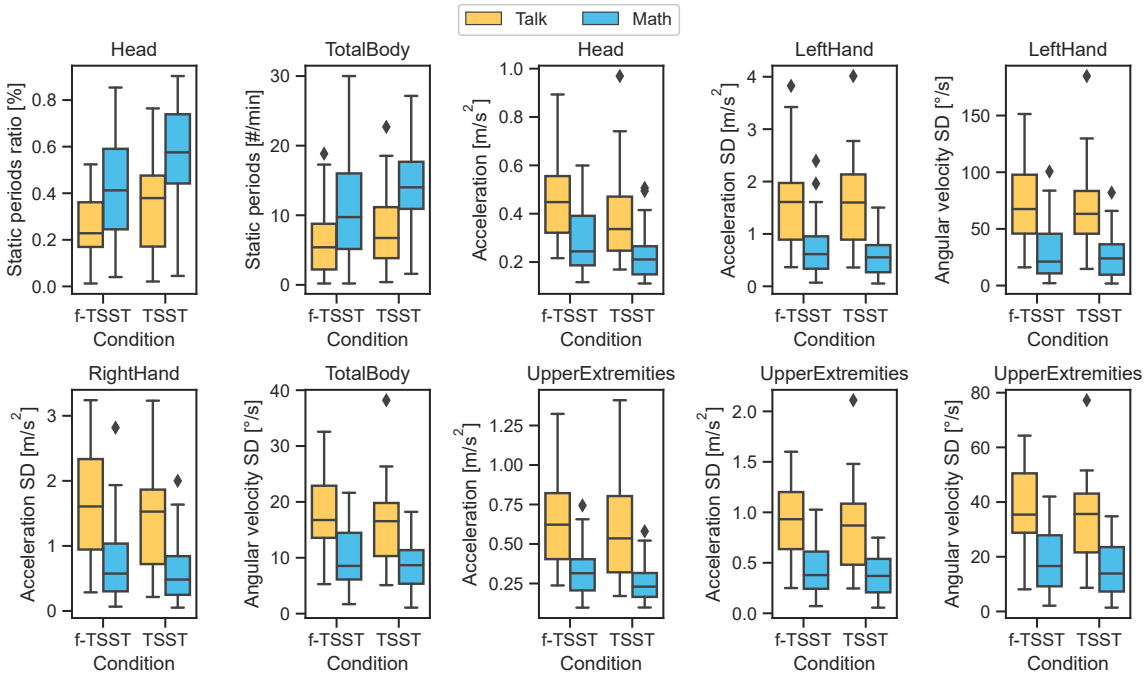

Figure 4.8: Motion feature differences between the (f-)TSST phases talk and math; selection by highest absolute t-value

As shown in Figure 4.8, there are various differences between the math and talk phases of (f-)TSST. For example, the ratio of static periods of the head are increased for the math part and the mean acceleration of the head is decreased for both conditions. For the total body, the number of static periods per minute is significantly increased for the talk part of both conditions. All in all, it can be concluded that there is considerably less body movement in the math part compared to the talk part. This could indicate that the results from the previous study by Richer et al. [Ric22] are over-optimistic, as their study protocol did not include a math part for the f-TSST.

Discussion

The motion and posture characteristics observed during the TSST are reflecting the freezing behaviour showed in previous studies e.g. [Roe17; Zee19]. Especially reduced head movement (quantified by reduced mean angular velocity, or increased mean and max static periods) seems to be an distinct marker for acute psychosocial stress. Furthermore, the head flexion angle was significantly decreased during the TSST, which is another promising measure for acute stress. Another body region, which was used to evaluate freezing in previous studies, is the chest or trunk (e.g. [Hag14]). The results from this work confirm these findings, as

the chest showed reduced mean angular velocity and more as well as longer static periods. Reduced motion was also be observed in the upper extremities as well as the total body. All in all, it can be concluded that defensive freezing behaviour is a promising marker for acute stress. The results from this section are limited by the fact that the evaluations were done between the conditions, although the condition is not directly related to the level of stress experienced by the participant. From previous work, as well as the results from this work it is well-known that about one third of the participants in TSST studies do not show a response in salivary cortisol levels [Dic04], and therefore could be considered as not stressed, which can have various reasons, e.g. long term stress that inhibits HPA axis activity [McL22].

In contrast to the previous study by Richer et al. [Ric22], the differences between the conditions were, on average, smaller, which could be explained by the improved study design. For the study in this work, the placebo-TSST mental arithmetic part was added to the f-TSST, which helped making the protocols more comparable, as posture and bodily motion highly differ between performing speech or mental arithmetic. This could be further investigated by a separate evaluation of the talk and math part, or a time-dependent approach, where motion and posture features are calculated in smaller time windows. Additionally, the preparatory phase could be taken into account to check if anticipation of the threatening situation does already affect bodily movements.

4.2.2 Gait & Mobility Tests

Two participants were excluded from the analysis of the gait and mobility tests due to problems with the MoCap recording. Therefore, results from $n = 39$ participants are reported.

TUG

The TUG did not show any significant effects. As shown in Figure 4.9, there are only minor differences between the conditions. To account for day to day differences, the features relative to Trial 0 have been calculated as shown in Figure A.1. This did not reveal any significant effects as well.

Gait Tests

The spatio-temporal features extracted from the 4×10 m gait tests are shown in Figures 4.10, and A.2. Similar to the TUG, the 4×10 m gait tests did not show any significant effects. Only small differences between the conditions can be found e.g. an decreased maximum sensor lift after the TSST at preferred speed (Figure 4.10). Since the results from the TUG as well as the 4×10 m gait tests did not look promising, these features were excluded from further analyses.

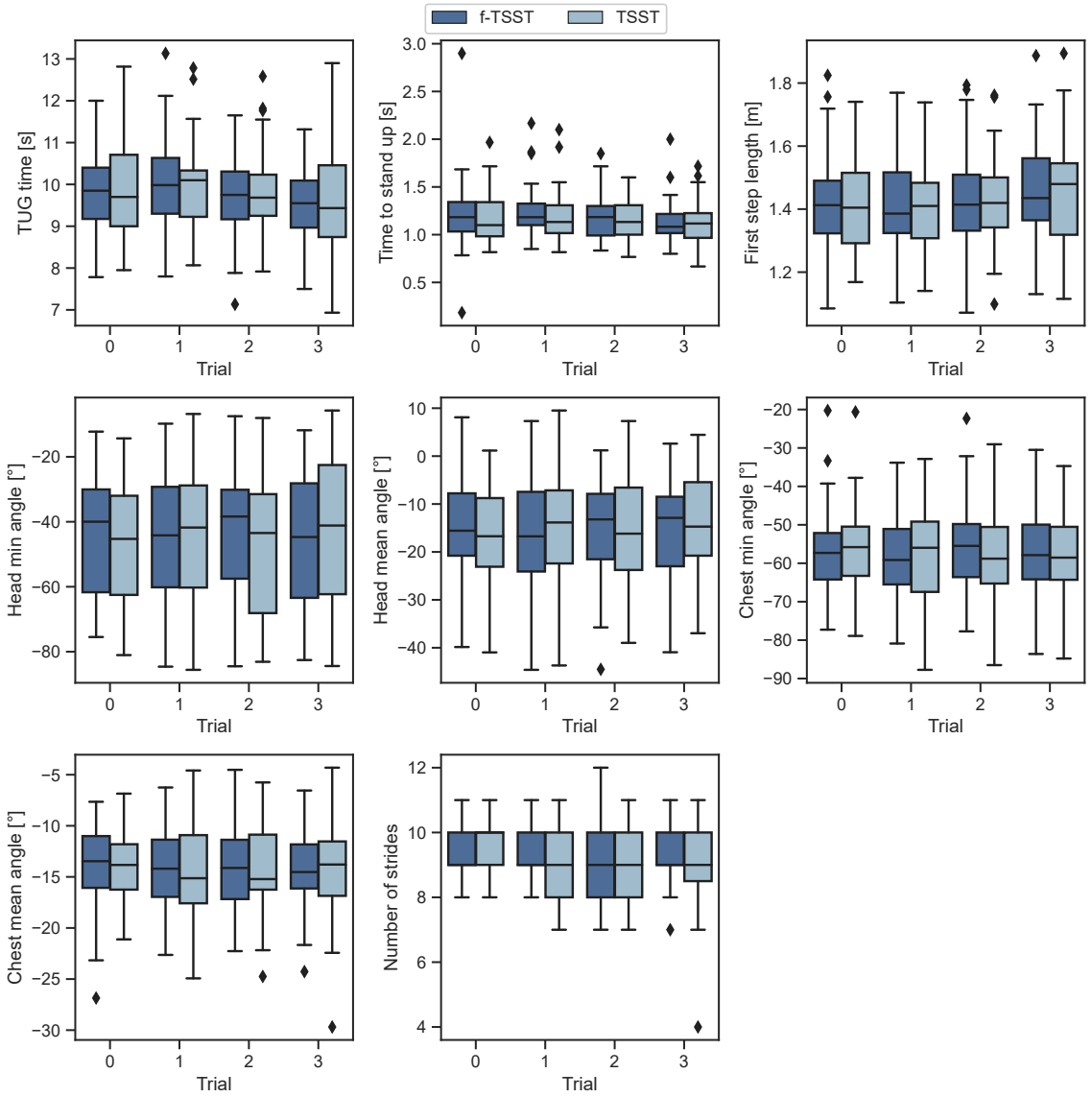

Figure 4.9: TUG features; for all participants and trials

Discussion

There are various possible reasons that the results from the TUG and 4×10 m gait tests did not show the beforehand expected changes from acute stress. In general, it is possible that an acute stress situation does not affect dynamic movements such as walking. From the observation of the study instructors, no alterations could be observed by the naked eye, indicating that these changes are minor. Nevertheless, there are a few limitations in the study design that should be addressed in future studies.

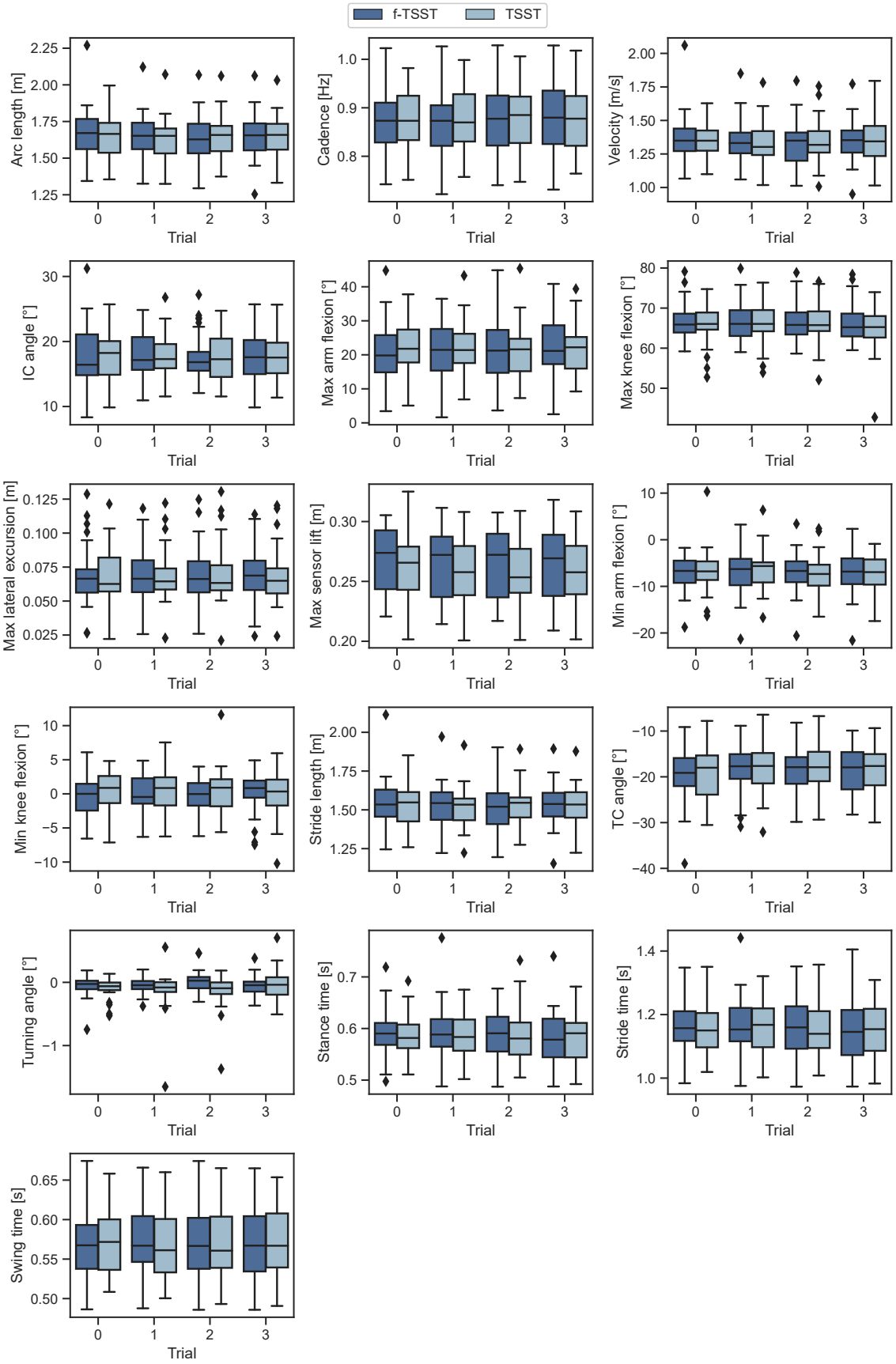

Figure 4.10: Spatiotemporal features; for all participants and trials

First of all, due to time constraints within the study design, the number iterations of the gait and mobility tests per trial was quite low. Therefore, it is possible that effects could not be observed. Secondly, the first trial of the gait & mobility tests (G_1) after the TSST could not be performed earlier than 10 min after TSST end (25 min relative to TSST start) due to timing conflicts with the questionnaires. Because the questionnaires should be completed right after the (f-)TSST to achieve comparability with previous TSST studies, it was decided to put the first trial of gait tests after the questionnaires. It is possible, that participants had the opportunity to process the negative experiences from the TSST by completing the questionnaires. Thus, the expected changes in dynamic movement due to the imminent threatening situation could probably not be observed.

In a study by Mascret et al., investigating the influence of TSST on basketball free throw performance, no effects on movement executions were found [Mas16]. Therefore, it is possible that no such effects on dynamic movements exist.

Additionally, the expected movement alterations at G_3 due to inflammatory responses are probably not showing yet, as 75 min relative to TSST start are a relatively short time to observe the rather slow inflammatory processes. In previous studies, the inflammatory marker Interleukin-6 (IL-6) showed a on ongoing increase about 2 h after the TSST e.g. [Ste01]. Hence, the last trial of the gait and mobility tests was probably performed too early to reveal any inflammatory effects. Furthermore, the inflammatory response following an acute stressor is a low-grade inflammation [Roh19]. As a consequence, the inflammatory stress on the individual is not that high which could be another explanation why there are no changes showing during the gait & mobility tests, in contrast to the findings of Lasselin et al. who induced acute inflammation pharmaceutical [Las20].

To summarize, future studies that assess the influence of acute stress on dynamic movements should perform gait and mobility tests right after the stress task. Additionally, to assess the consequences of acute stress, such as low-grade systemic inflammation, the time between the TSST and the last trial should be stretched to at least 105 min after TSST start (90 min after TSST end). Furthermore, future work could look into different types of gait and mobility tests which could be better suited assessing the bodily motions after an acute stressor.

4.3 Backward Multiple Linear Regression

An explained variance of 80 % was achieved with $n = 8$ PCA components for head and chest, and with $n = 7$ components for upper extremities and total body, respectively. For predicting Δc_{max} , the highest explained variance (26.8 %) was achieved using total body features with four components (Table 4.3). For PASA-Challenge, upper extremities achieved an explained variance of 15.6 % (Table B.7). PANAS-NegativeAffect was best predicted by features of the head, achieving an explained variance of 12.7 % with 2 components (Table B.8). 16.6 % of the variance of PANAS-PositiveAffect score, and 30.5 % of the variance of PASA-Threat score could be explained by a model obtained from chest features (Tables B.9 and B.10).

Table 4.3: Results of linear regression predicting Δc_{max} with total body features; β: standardized regression coefficient; σ: standard error; adj.: adjusted

components	β	σ	t	p	R^2	adj. R^2
TotalBody_PCA_1	0.111	0.046	2.416	0.021	0.345	0.268
TotalBody_PCA_2	-0.076	0.047	-1.604	0.118	0.345	0.268
TotalBody_PCA_3	-0.181	0.069	-2.615	0.013	0.345	0.268
TotalBody_PCA_6	0.167	0.103	1.631	0.112	0.345	0.268

When using PCA components from multiple body parts to predict endocrine and self-reported measures, two of the components were omitted because of high multicollinearity, resulting in a total of 28 components from four different body parts / body part groups. For PASA-Challenge and Threat, the stepwise backward linear regression was able to reduce the number of components to 11 and 9, achieving an explained variance of 43.9 % and 33.7 %, respectively (Tables 4.4 and B.11) . Δc_{max} could be predicted with an explained variance of 61.4 % (15 components; Table 4.5).

In a previous work by Lasselin et al. [Las20], the authors achieved an explained variance of 60 % to predict motion alterations from body temperature, sickness symptoms, back pain, and IL-6 concentration with SBMLR. Thus, the results of this thesis of more than 60 % explained variance for Δc_{max} are on a comparable level. Although the results from the SBMLR are quite promising, the model obtained from this approach probably does not generalize well as there is no validation on a separate test set. Additionally, the approach of performing a PCA leads to difficulties in interpreting results as the PCA components cannot be directly connected to the observed motion alterations.

Table 4.4: Results of linear regression predicting PASA-Challenge with features of head, chest, upper extremities, and total body; β: standardized regression coefficient; σ: standard error; adj.: adjusted

components	β	σ	t	p	R^2	adj. R^2
TotalBody_PCA_2	0.558	0.139	4.025	0.000	0.602	0.439
TotalBody_PCA_3	-0.528	0.146	-3.628	0.001	0.602	0.439
TotalBody_PCA_4	0.315	0.090	3.509	0.002	0.602	0.439
TotalBody_PCA_5	-0.231	0.127	-1.817	0.080	0.602	0.439
TotalBody_PCA_6	0.396	0.123	3.233	0.003	0.602	0.439
Chest_PCA_2	-0.144	0.116	-1.248	0.223	0.602	0.439
Chest_PCA_3	-0.224	0.097	-2.304	0.029	0.602	0.439
Chest_PCA_4	-0.170	0.099	-1.711	0.099	0.602	0.439
UpperExtremities_PCA_1	0.474	0.142	3.330	0.003	0.602	0.439
Head_PCA_2	0.320	0.080	4.013	0.000	0.602	0.439
Head_PCA_6	-0.161	0.087	-1.845	0.076	0.602	0.439

Table 4.5: Results of linear regression predicting Δc_{max} with features of head, chest, upper extremities, and total body; β: standardized regression coefficient; σ: standard error; adj.: adjusted

components	β	σ	t	p	R^2	adj. R^2
TotalBody_PCA_1	-0.747	0.185	-4.045	0.001	0.767	0.614
TotalBody_PCA_2	-0.854	0.127	-6.739	0.000	0.767	0.614
TotalBody_PCA_5	-0.416	0.136	-3.071	0.005	0.767	0.614
Chest_PCA_4	-0.305	0.085	-3.598	0.002	0.767	0.614
Chest_PCA_5	-0.106	0.072	-1.459	0.158	0.767	0.614
Chest_PCA_6	0.295	0.084	3.530	0.002	0.767	0.614
Chest_PCA_7	0.371	0.105	3.536	0.002	0.767	0.614
Chest_PCA_8	0.228	0.122	1.867	0.075	0.767	0.614
UpperExtremities_PCA_1	0.394	0.103	3.842	0.001	0.767	0.614
UpperExtremities_PCA_2	1.243	0.258	4.815	0.000	0.767	0.614
UpperExtremities_PCA_3	0.515	0.135	3.801	0.001	0.767	0.614
UpperExtremities_PCA_4	0.198	0.108	1.828	0.081	0.767	0.614
UpperExtremities_PCA_5	0.371	0.135	2.750	0.011	0.767	0.614
Head_PCA_2	-0.316	0.073	-4.316	0.000	0.767	0.614
Head_PCA_4	0.166	0.082	2.020	0.055	0.767	0.614

4.4 Classification

The classification of the conditions from motion features during (f-)TSST achieved a mean accuracy of 74.3 $\pm$ 4.2 % for the best performing pipeline using the following parameters:

- Scaling: StandardScaler
- Feature selection: SelectKBest (k = 28)
- Classifier: DecisionTree

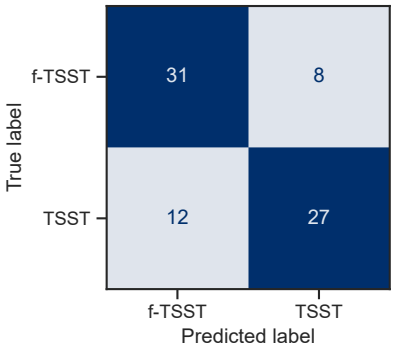

Figure 4.11: Confusion matrix condition classification

In Figure 4.11, the confusion matrix for the best performing pipeline is displayed, an overview of the results for the different pipelines is given in Table 4.6. When evaluating the best performing pipeline separately for the condition orders, it can be seen that TSST-first could be classified with a considerably higher accuracy (81.6 % vs. 67.5 %). The confusion matrices separated by condition orders are shown in Figure 4.12.

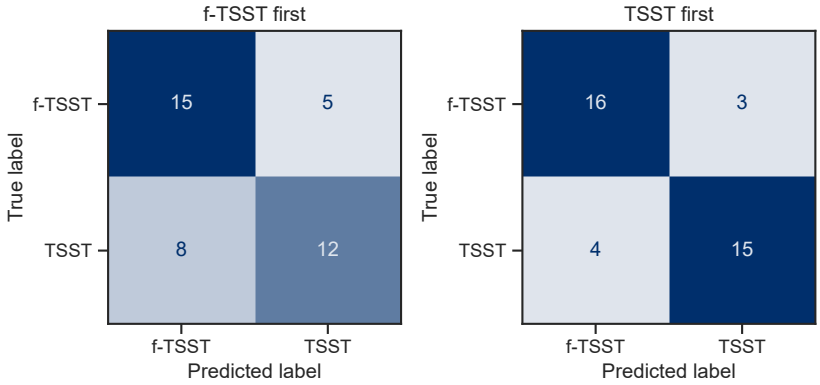

Figure 4.12: Confusion matrix condition classification; separated by condition order

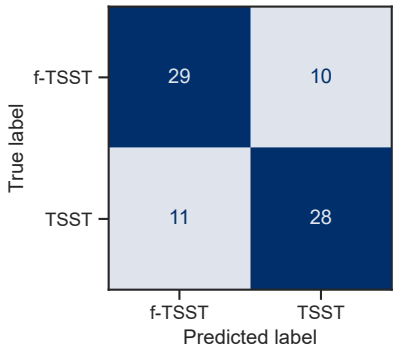

Figure 4.13: Confusion matrix condition classification from features separated by phase

Because of the large differences between the math and talk phases of the (f-)TSST, classification was performed for features separated by phases as well. The best performing pipeline with StandardScaler, RFE, and RandomForestClassifier achieved a mean test accuracy of 73.2 ± 5.5 %. The classification performance could not be boosted by calculating the features separately for the phases. The confusion matrix for this is shown in Figure 4.13.

Table 4.6: Comparison of different ML pipelines; accuracy ± SD; best performing pipeline per classifier highlighted

Feature selection	RFE		SelectKBest	
Scaling	MinMax	Standard	MinMax	Standard
Classification				
KNeighborsClassifier	58.2 ± 16.4	61.6 ± 4.8	62.7 ± 5.4	**63.9 ± 7.1**
SVC	60.2 ± 6.3	51.4 ± 8.4	**62.7 ± 5.4**	58.8 ± 5.0
DecisionTreeClassifier	65.4 ± 2.8	56.6 ± 13.3	66.4 ± 7.3	**74.3 ± 4.2**
AdaBoostClassifier	65.5 ± 8.8	61.8 ± 5.6	66.4 ± 8.3	**67.9 ± 5.9**
RandomForestClassifier	66.4 ± 9.2	**69.3 ± 6.9**	64.1 ± 2.4	66.2 ± 12.2

The small standard deviation achieved for the classification accuracy could be a sign that the classification model is quite robust. When comparing these results to previous studies by Aigrain et al. and Richer et al. [Ric22], who achieved accuracy scores of 77 % and 85 %, the results of this work are slightly worse. As explained in Section 4.2.1, the decrease in accuracy, compared to the previous work from Richer et al., is expected as they did not include any math part in the f-TSST protocol, and therefore did not have good comparability between the conditions. When taking into account that Aigrain et al. used a multi-modal approach instead of just one modality, the results from this work are quite promising, as extending the model to multiple modalities is likely to increase the performance.

4.5 ML-Based Regression

ML-based regression using PASA-Challenge and Threat as a dependent variable performed very poorly, with negative R^2 values (-0.617, and -1.615, respectively) and therefore will not be discussed in detail. Negative R^2 values appear when the residual sum of squares approaches the total sum of squares, meaning that the explained variance of the dependent variable is very low or negligible.

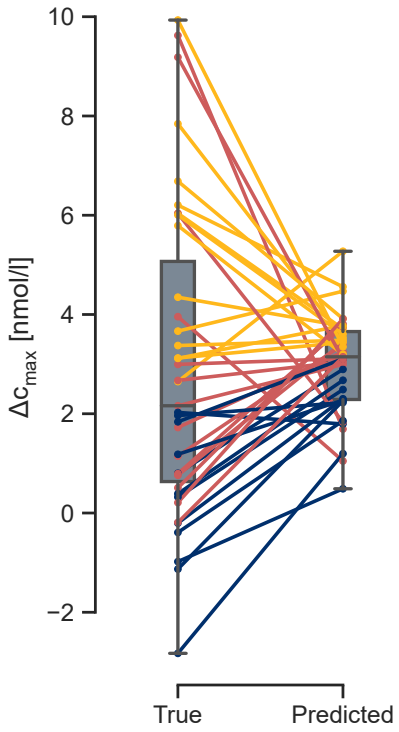

Figure 4.14: Regression results Δc_{max} ; yellow: true and predicted value over the respective median; blue: true and predicted value lower than the respective median; red: true and predicted values not on the same side of the respective median

The ML-based regression using Δc_{max} as a dependent variable yielded an R^2 value of 0.063 ± 0.129 and a mean absolute error (MAE) of $3.10 \pm 2.58\,\mathrm{nmol\,l^{-1}}$ with the best performing pipeline using $\mathrm{MinMaxScaler}$, RFE, and $\mathrm{RandomForestRegressor}$. Neither optimizing for the mean absolute error nor considering the features from the (f-)TSST phases separately improved regression performance (R^2: -0.010, and 0.051, respectively).

Although the R^2 value is quite low, a further analysis revealed a promising trend, as shown in Figure 4.14. Most of the samples which are higher than the median of the true Δc_{max} values are predicted to be above the median of the predicted Δc_{max} values. 65.4 % of the samples are predicted to be in right half. This indicates that with more samples, or a multi-modal approach, regression performance could possibly be boosted considerably.

As mentioned before, these results are not really comparable to the results of the SBMLR, as the SBMLR tends to overfit to the data as no independent test set is used to validate the generalizability of the model.

4.6 General Discussion & Limitations

All in all, the results indicate that stress can be reliably detected from body posture and movement. Statistical evaluation of the features, as well as classification of the stressed vs. non-stressed conditions, and SBMLR could reproduce results from previous work, e.g. [Ric22]. Thus, the results from this work support the finding that freezing behavior could be a distinct marker for the acute stress reaction.

The f-TSST, although the results for cortisol support the finding that it does not activate the HPA axis, is not very standardized. In contrast to the TSST, the f-TSST was used considerably less in previous work. Thus, the expertise on how to perform a standardized f-TSST is limited. Nevertheless, it should be pointed out that this new protocol, combining the f-TSST and the placebo-TSST, is an approach with provides better comparability, and should be therefore further investigated in future studies. The addition of the math part, although providing better comparability to the TSST, was seen critically by members of the panel. Five minutes of mental arithmetic, even though it was a quite easy task, seemed to still induce stress among participants, who see mental arithmetic as their weak point. For participants, who were confident in their math skills, members of the panel reported that participants seemed to be annoyed by the length of the simple task, as it can get quite boring to count in steps of 15 for five minutes. Further studies should investigate other possibilities of obtaining a non-stressing control condition that does not activate the HPA axis while concurrently maintaining comparability and omitting the possible confounding effects of the math part.

Working with an IMU-based system posed several limitations on the results. In general, IMU-based systems have the problem of drifting. Although large drifting effects were not observed in the data, small drifts happened frequently. The placement of the sensors should be compensated by the Xsens calibration software but can never be exactly reproduced. Additionally, the quality of the calibration varied a lot if participants did not hold the static pose for long enough. The velcro straps of the Xsens system do a decent job holding the sensors at their place. Nevertheless, from time to time the straps did not stay at their position,

especially when the velcro straps got stuck to each other. A possible solution could be to use an maker-based, optical MoCap system in future studies, which offers more precision, but comes with the drawback of increased costs.

Another limitation of the results could be that the usage of the MoCap system is causing participants to act non-naturally. Especially on the first day of the study participants were not used to have several sensors as well as a tight shirt on their body, which could be a further explanation for the condition order effects described in Section 4.1.1. This could be solved by changing to a more unobtrusive system to quantify bodily motions, e.g. a camera or radar-based tracking system.

Chapter 5

Conclusion & Outlook

The results of this work are quite promising. Especially exploring the freezing behavior in the TSST with a larger study population could be the foundation of future work. The TSST as the gold standard for acute stress induction in a laboratory environment proved to be a well-functioning tool for investigating psychosocial stress responses. Both in the endocrinological measures and the measures obtained from self-report, it could be seen that acute stress induction with the TSST was performed successfully for most of the participants. The modified version of the f-TSST that was used for the first time, combining the f-TSST with the math part of the placebo-TSST proved to provide better comparability between the stress and non-stress conditions, while keeping HPA axis activation low. However, it has to be further investigated, which influences the addition of the math part has on the individual experience of the participants.

The expected defensive freezing behavior due to acute stress could be seen especially for the head, trunk, and upper extremities, as well as the total body. There were no effects observed regarding potential gender differences in body posture and movement during acute stress. Additionally, it was shown that there is probably only very minor effects of acute stress on dynamic movement performed after an acute stress situation or the standardized gait test was performed too late after the end of the stressful situation. If low-grade inflammation, as induced by acute stress, lead to alterations on body posture and movement could not be answered with this work. Possible explanations, why no movement alterations could be observed, could be that the inflammatory response is too weak to influence body posture and movement, or that the gait and mobility tests were performed too early.

The classification of non-stress vs. stress conditions achieved an accuracy of 74 %, which is comparable to previous work and promising for detecting acute stress in a laboratory environment. However, at the same time, it shows that for achieving reliable, contactless, "in the wild", acute stress detection there is still a long way to go. Especially predicting the endocrine stress marker cortisol seems like a particular difficult task, although the results from the SBMLR looked promising.

The resulting dataset, obtained through this study, is quite extensive. Additional to the MoCap data, two cameras recorded the (f-)TSST, and various self-reports assessing psychological traits and states have been completed by the participants. From this, various further evaluations could be performed. For example, similar motion features to those extracted from MoCap data could also be computed from RGB-D videos obtained by the Microsoft Azure Kinect camera, thus allowing to first validate both approaches against each other, and, potentially, replacing the MoCap suit by a more contactless modality. From the camera imagery, activation of facial action units, according to the FACS [Ekm78], could be extracted to investigate facial features during acute stress. Additionally, α-amylase as well as CRP were not part of the evaluation yet. Psychological questionnaires could reveal more relations between bodily movement during stress and e.g. body-esteem (obtained from the Body Esteem Scale (BES)). Furthermore, the data could be combined with the data from a previous study with a similar protocol to achieve better generalization.

In future studies, the potential focus could be on micro movements instead of bodily motion and posture. As mentioned before, heart rate parameters are promising for the detection of acute stress. In addition, electrodermal activity could be a useful measure for quantifying acute stress. The goal should be to combine the novel sensor technology developed in other EmpkinS [Emp22] subprojects with the stress protocol used in this work. This includes several contactless systems, e.g. a radar-based system for measuring heart rate and respiration, a radar-based system for estimating body posture and movement, as well as a sensor for measuring micro-structural skin changes. Potential multimodal approaches, combining motion features with e.g. facial features, heart rate (variability), or electrodermal activity could lead to a more robust approach.

Additionally, the usage of a more natural stress protocol, outside of the laboratory, could be the topic of future works. The ultimate goal is to achieve a comprehensive understanding of stressful situations and and the transition of (repeated) acute stress into chronic stress outside the laboratory, which can be used to develop interventions that are based on data obtained with non-contact sensors. Research into psycho-motoric models could lay the foundations for characterizing the internal states of humans during an acute, psychosocial stress reaction from purely externally detectable parameters for the first time.

List of Figures

List of Tables

Bibliography

[Abe19] Luca Abel, Robert Richer, Arne Küderle, Stefan Gradl, Bjoern M. Eskofier, and Nicolas Rohleder. "Classification of Acute Stress-Induced Response Patterns". In: *Proceedings of the 13th EAI International Conference on Pervasive Computing Technologies for Healthcare - PervasiveHealth'19*. New York, New York, USA: ACM Press, 2019, pp. 366–370. ISBN: 978-1-4503-6126-2. DOI: 10.1145/3329189.3329231. URL: http://dl.acm.org/citation.cfm?doid=3329189.3329231.

[Aig15] Jonathan Aigrain, Severine Dubuisson, Marcin Detyniecki, and Mohamed Chetouani. "Person-specific behavioural features for automatic stress detection". en. In: *2015 11th IEEE International Conference and Workshops on Automatic Face and Gesture Recognition (FG)*. Ljubljana: IEEE, May 2015, pp. 1–6. ISBN: 978-1-4799-6026-2. DOI: 10.1109/FG.2015.7284844. URL: http://ieeexplore.ieee.org/document/7284844/ (visited on 05/20/2021).

[All14] Andrew P. Allen, Paul J. Kennedy, John F. Cryan, Timothy G. Dinan, and Gerard Clarke. "Biological and psychological markers of stress in humans: Focus on the Trier Social Stress Test". en. In: *Neuroscience & Biobehavioral Reviews* 38 (Jan. 2014), pp. 94–124. ISSN: 0149-7634. DOI: 10.1016/j.neubiorev.2013.11.005. URL: https://www.sciencedirect.com/science/article/pii/S0149763413002728 (visited on 05/20/2022).

[All17] Andrew P. Allen, Paul J. Kennedy, Samantha Dockray, John F. Cryan, Timothy G. Dinan, and Gerard Clarke. "The Trier Social Stress Test: Principles and practice". en. In: *Neurobiology of Stress*. SI:Stressors in animals 6 (Feb. 2017), pp. 113–126. ISSN: 2352-2895. DOI: 10.1016/j.ynstr.2016.11.001. URL: https://www.sciencedirect.com/science/article/pii/S2352289516300224 (visited on 04/25/2022).

[APA19] APA. "Stress in America™ 2019". en. In: *American Psychology Association* (2019).

[Atk04] Anthony P Atkinson, Winand H Dittrich, Andrew J Gemmell, and Andrew W Young. "Emotion Perception from Dynamic and Static Body Expressions in Point-Light and Full-Light Displays". en. In: *Perception* 33.6 (June 2004). Publisher: SAGE Publications Ltd STM, pp. 717–746. ISSN: 0301-0066. DOI: 10.1068/p5096. URL: https://doi.org/10.1068/p5096 (visited on 04/25/2022).

[Axe18] John Axelsson, Tina Sundelin, Mats J. Olsson, Kimmo Sorjonen, Charlotte Axelsson, Julie Lasselin, and Mats Lekander. "Identification of acutely sick people and facial cues of sickness". en. In: *Proc. R. Soc. B.* 285.1870 (Jan. 2018). tex.ids: Axelsson2018 publisher: royalsocietypublishing.org, p. 20172430. ISSN: 0962-8452, 1471-2954. DOI: 10.1098/rspb.2017.2430. URL: https://royalsocietypublishing.org/doi/10.1098/rspb.2017.2430 (visited on 10/18/2020).

[Bar11] Jens Barth, Jochen Klucken, Patrick Kugler, Thomas Kammerer, Ralph Steidl, Jürgen Winkler, Joachim Hornegger, and Björn Eskofier. "Biometric and mobile gait analysis for early diagnosis and therapy monitoring in Parkinson's disease". In: *2011 Annual International Conference of the IEEE Engineering in Medicine and Biology Society*. ISSN: 1558-4615. Aug. 2011, pp. 868–871. DOI: 10.1109/IEMBS.2011.6090226.

[Bid20] Christel Bidet-Ildei, Arnaud Decatoire, and Sandrine Gil. "Recognition of Emotions From Facial Point-Light Displays". In: *Frontiers in Psychology* 11 (2020). ISSN: 1664-1078. URL: https://www.frontiersin.org/article/10.3389/fpsyg.2020.01062 (visited on 05/20/2022).

[Bla86] Robert J. Blanchard, Kevin J. Flannelly, and D. Caroline Blanchard. "Defensive behaviors of laboratory and wild Rattus norvegicus." In: *Journal of Comparative Psychology* 100.2 (1986). Place: US Publisher: American Psychological Association, pp. 101–107. ISSN: 1939-2087. DOI: 10.1037/0735-7036.100.2.101.

[Boo98] R Thomas Boone and Joseph Cunningham. "Children's Decoding of Emotion in Expressive Body Movement: The Development of Cue Attunement". In: *Developmental psychology* 34 (Oct. 1998), pp. 1007–16. DOI: 10.1037/0012-1649.34.5.1007.

[Cal14] Manuel G. Calvo, Aida Gutiérrez-García, Andrés Fernández-Martín, and Lauri Nummenmaa. "Recognition of Facial Expressions of Emotion is Related to their Frequency in Everyday Life". en. In: *J Nonverbal Behav* 38.4 (Dec. 2014), pp. 549–567. ISSN: 1573-3653. DOI: 10.1007/s10919-014-0191-3. URL: https://doi.org/10.1007/s10919-014-0191-3 (visited on 05/20/2022).

[Cam04] Antonio Camurri, Barbara Mazzarino, Matteo Ricchetti, Renee Timmers, and Gualtiero Volpe. "Multimodal Analysis of Expressive Gesture in Music and Dance Performances". en. In: *Gesture-Based Communication in Human-Computer Interaction*. Ed. by Antonio Camurri and Gualtiero Volpe. Lecture Notes in Computer Science. Berlin, Heidelberg: Springer, 2004, pp. 20–39. ISBN: 978-3-540-24598-8. DOI: 10.1007/978-3-540-24598-8_3.

[Car16] Roger Carpenter. "A Review of Instruments on Cognitive Appraisal of Stress". en. In: *Archives of Psychiatric Nursing* 30.2 (Apr. 2016), pp. 271–279. ISSN: 0883-9417. DOI: 10.1016/j.apnu.2015.07.002. URL: https://www.sciencedirect.com/science/article/pii/S0883941715001429 (visited on 05/15/2022).

[Coh07] Sheldon Cohen, Denise Janicki-Deverts, and Gregory E. Miller. "Psychological Stress and Disease". In: *JAMA* 298.14 (Oct. 2007), pp. 1685–1687. ISSN: 0098-7484. DOI: 10.1001/jama.298.14.1685. URL: https://doi.org/10.1001/jama.298.14.1685 (visited on 05/02/2022).

[Dic04] Sally S. Dickerson and Margaret E. Kemeny. "Acute stressors and cortisol responses: A theoretical integration and synthesis of laboratory research". In: *Psychological Bulletin* 130.3 (2004). ISBN: 0033-2909 (Print)\n0033-2909 (Linking), pp. 355–391. ISSN: 00332909. DOI: 10.1037/0033-2909.130.3.355. URL: 10.1037/0033-2909.130.3.355.

[Ekm78] Paul Ekman and Wallace V Friesen. *Facial action coding system*. English. OCLC: 605256401. Palo Alto (Calif.): Consulting Psychologists Press, 1978.

[Emp22] EmpkinS. *EmpkinS – Website für den SFB-Antrag Empathokinästhetische Sensorik*. de. 2022. URL: https://empkins.de/ (visited on 01/04/2022).

[Fel20] Ron Feldman, Shaul Schreiber, and Ella Been. "Gait, Balance and Posture in Major Mental Illnesses: Depression, Anxiety and Schizophrenia". In: *Austin Med Sci* 5.1 (2020). tex.ids: Feldman2020a publisher: researchgate.net, p. 1039.

[Fol10] Paul Foley and Clemens Kirschbaum. "Human hypothalamus-pituitary-adrenal axis responses to acute psychosocial stress in laboratory settings". eng. In: *Neurosci Biobehav Rev* 35.1 (Sept. 2010), pp. 91–96. ISSN: 1873-7528. DOI: 10.1016/j.neubiorev.2010.01.010.

[Gaa09] J. Gaab. "PASA – Primary Appraisal Secondary Appraisal - Ein Fragebogen zur Erfassung von situations-bezogenen kognitiven Bewertungen". deu. In: *Verhaltenstherapie* 19.2 (July 2009). Number: 2 Publisher: Karger, pp. 114–115. ISSN: 1016-6262. DOI: 10.1159/000223610. URL: https://www.zora.uzh.ch/id/eprint/24570/ (visited on 04/19/2022).

[Gel12] Andrew Gelman, Jennifer Hill, and Masanao Yajima. "Why We (Usually) Don't Have to Worry About Multiple Comparisons". In: *Journal of Research on Educational Effectiveness* 5.2 (Apr. 2012), pp. 189–211. ISSN: 1934-5747. DOI: 10.1080/19345747.2011.618213. (Visited on 05/03/2022).

[Gla16] Thomas E. Gladwin, Mahur M. Hashemi, Vanessa van Ast, and Karin Roelofs. "Ready and waiting: Freezing as active action preparation under threat". en. In: *Neuroscience Letters* 619 (Apr. 2016), pp. 182–188. ISSN: 0304-3940. DOI: 10.1016/j.neulet.2016.03.027. URL: https://www.sciencedirect.com/science/article/pii/S0304394016301574 (visited on 05/04/2022).

[Hag14] Muriel A. Hagenaars, Karin Roelofs, and John F. Stins. "Human freezing in response to affective films". en. In: *Anxiety, Stress, & Coping* 27.1 (Jan. 2014), pp. 27–37. ISSN: 1061-5806, 1477-2205. DOI: 10.1080/10615806.2013.809420. URL: http://www.tandfonline.com/doi/abs/10.1080/10615806.2013.809420 (visited on 10/17/2020).

[Ham20] Ajna Hamidovic, Kristina Karapetyan, Fadila Serdarevic, So Hee Choi, Tory Eisenlohr-Moul, and Graziano Pinna. "Higher Circulating Cortisol in the Follicular vs. Luteal Phase of the Menstrual Cycle: A Meta-Analysis". In: *Frontiers in Endocrinology* 11 (2020). ISSN: 1664-2392. URL: https://www.frontiersin.org/article/10.3389/fendo.2020.00311 (visited on 05/18/2022).

[Has21] Mahur M. Hashemi, Wei Zhang, Reinoud Kaldewaij, Saskia B. J. Koch, Annika Smit, Bernd Figner, Rosa Jonker, Floris Klumpers, and Karin Roelofs. "Human defensive freezing: Associations with hair cortisol and trait anxiety". en. In: *Psychoneuroendocrinology* 133 (Nov. 2021), p. 105417. ISSN: 0306-4530. DOI: 10.1016/j.psyneuen.2021.105417. URL: https://www.sciencedirect.com/science/article/pii/S0306453021002912 (visited on 04/26/2022).

[Het09] S. Het, N. Rohleder, D. Schoofs, C. Kirschbaum, and O.T. Wolf. "Neuroendocrine and psychometric evaluation of a placebo version of the 'Trier Social Stress Test'". en. In: *Psychoneuroendocrinology* 34.7 (Aug. 2009), pp. 1075–1086. ISSN: 03064530. DOI: 10.1016/j.psyneuen.2009.02.008. URL: https://linkinghub.elsevier.com/retrieve/pii/S0306453009000614 (visited on 01/18/2022).

[Jar18] Delaram Jarchi, James Pope, Tracey K. M. Lee, Larisa Tamjidi, Amirhosein Mirzaei, and Saeid Sanei. "A Review on Accelerometry-Based Gait Analysis and Emerging Clinical Applications". In: *IEEE Reviews in Biomedical Engineering* 11 (2018). Conference Name: IEEE Reviews in Biomedical Engineering, pp. 177–194. ISSN: 1941-1189. DOI: 10.1109/RBME.2018.2807182.

[Kan15] Christoph Kanzler, Jens Barth, Alexander Rampp, Heiko Schlarb, Franz Rott, Jochen Klucken, and Bjoern Eskofier. "Inertial Sensor based and Shoe Size Independent Gait Analysis including Heel and Toe Clearance Estimation". In: vol. 2015. Aug. 2015. DOI: 10.1109/EMBC.2015.7319618.

[Kap05] A. Kapur, A. Kapur, N. Virji-Babul, G. Tzanetakis, and P. Driessen. "Gesture-Based Affective Computing on Motion Capture Data". In: *ACII*. 2005. DOI: 10.1007/11573548_1.

[Kar13] Michelle Karg, Ali-Akbar Samadani, Rob Gorbet, Kolja Kühnlenz, Jesse Hoey, and Dana Kulić. "Body Movements for Affective Expression: A Survey of Automatic Recognition and Generation". In: *IEEE Transactions on Affective Computing* 4.4 (Oct. 2013). Conference Name: IEEE Transactions on Affective Computing, pp. 341–359. ISSN: 1949-3045. DOI: 10.1109/T-AFFC.2013.29.

[Kaz79] Alan E. Kazdin. "Unobtrusive measures in behavioral assessment". In: *J Appl Behav Anal* 12.4 (1979), pp. 713–724. ISSN: 0021-8855. DOI: 10.1901/jaba.1979.12-713. URL: https://www.ncbi.nlm.nih.gov/pmc/articles/PMC1311490/ (visited on 01/12/2022).

[Kir93] Clemens Kirschbaum, Karl-Martin Pirke, and Dirk H. Hellhammer. "The 'Trier Social Stress Test' – A Tool for Investigating Psychobiological Stress Responses in a Laboratory Setting". In: *Neuropsychobiology*. Vol. 28. Issue: 1-2 ISSN: 0302282X. 1993, pp. 76–81. ISBN: 978-0-87421-656-1. DOI: 10.1159/000119004.

[Kwa17] Sang Gyu Kwak and Jong Hae Kim. "Central limit theorem: the cornerstone of modern statistics". In: *Korean J Anesthesiol* 70.2 (Apr. 2017), pp. 144–156. ISSN: 2005-6419. DOI: 10.4097/kjae.2017.70.2.144. URL: https://www.ncbi.nlm.nih.gov/pmc/articles/PMC5370305/ (visited on 05/21/2022).

[Las20] J. Lasselin, T. Sundelin, P.M. Wayne, M.J. Olsson, S. Paues Göranson, J. Axelsson, and M. Lekander. "Biological motion during inflammation in humans". en. In: *Brain, Behavior, and Immunity* 84 (Feb. 2020). tex.ids= Lasselin2019, Lasselin2020a publisher: Elsevier Inc., pp. 147–153. ISSN: 08891591. DOI: 10.1016/j.bbi.2019.11.019. URL: 10.1016/j.bbi.2019.11.019 (visited on 10/17/2020).

[Lup14] Sarah B. Lupis, Michelle Lerman, and Jutta M. Wolf. "Anger responses to psychosocial stress predict heart rate and cortisol stress responses in men but not women". In: *Psychoneuroendocrinology* 49 (Nov. 2014), pp. 84–95. ISSN: 0306-4530. DOI: 10.1016/j.psyneuen.2014.07.004. URL: https://www.ncbi.nlm.nih.gov/pmc/articles/PMC4165699/ (visited on 04/26/2022).

[Mas16] Nicolas Mascret, Jorge Ibáñez-Gijón, Vincent Bréjard, Martinus Buekers, Rémy Casanova, Tanguy Marqueste, Gilles Montagne, Guillaume Rao, Yannick Roux, and François Cury. "The Influence of the 'Trier Social Stress Test' on Free Throw Performance in Basketball: An Interdisciplinary Study". en. In: *PLOS ONE* 11.6 (June 2016). Publisher: Public Library of Science, e0157215. ISSN: 1932-6203. DOI: 10.1371/journal.pone.0157215. URL: https://journals.plos.org/plosone/article?id=10.1371/journal.pone.0157215 (visited on 05/26/2022).

[McL22] Carly McLaughlin, Robert Schutze, Craig Pennell, David Henley, Monique Robinson, Leon Straker, and Anne Smith. "The anticipatory response to stress and symptoms of depression and anxiety in early adulthood". en. In: *Psychoneuroendocrinology* 136 (Feb. 2022), p. 105605. ISSN: 0306-4530. DOI: 10.1016/j.psyneuen.2021.105605. URL: https://www.sciencedirect.com/science/article/pii/S0306453021004790 (visited on 05/20/2022).

[OCo21] Daryl B. O'Connor, Julian F. Thayer, and Kavita Vedhara. "Stress and Health: A Review of Psychobiological Processes". In: *Annual Review of Psychology* 72.1 (2021). _eprint: https://doi.org/10.1146/annurev-psych-062520-122331, pp. 663–688. DOI: 10.1146/annurev-psych-062520-122331. URL: https://doi.org/10.1146/annurev-psych-062520-122331 (visited on 01/03/2022).

[Pis18] Katarzyna Pisanski, Aleksander Kobylarek, Luba Jakubowska, Judyta Nowak, Amelia Walter, Kamil Błaszczyński, Magda Kasprzyk, Krystyna Łysenko, Irmina Sukiennik, Katarzyna Piątek, Tomasz Frackowiak, and Piotr Sorokowski. "Multimodal stress detection: Testing for covariation in vocal, hormonal and physiological responses to Trier Social Stress Test". en. In: *Hormones and Behavior* 106 (Nov. 2018). tex.ids: Pisanski2018, pp. 52–61. ISSN: 0018506X. DOI: 10.1016/j.yhbeh.2018.08.014. URL: 10.1016/j.yhbeh.2018.08.014 (visited on 10/18/2020).

[Pod91] Diane Podsiadlo and Sandra Richardson. "The Timed "Up & Go": A Test of Basic Functional Mobility for Frail Elderly Persons". en. In: *Journal of the American Geriatrics Society* 39.2 (1991), pp. 142–148. ISSN: 1532-5415. DOI: 10.1111/j.1532-5415.1991.tb01616.x. URL: https://onlinelibrary.wiley.com/doi/abs/10.1111/j.1532-5415.1991.tb01616.x (visited on 01/17/2022).

[Pol21] Ian Polanowski. "Work-related stress, anxiety or depression statistics in Great Britain, 2021". en. In: *UK Health Safety* (2021).

[Pru03] Jens C. Pruessner, Clemens Kirschbaum, Gunther Meinlschmid, and Dirk H. Hellhammer. "Two formulas for computation of the area under the curve represent

measures of total hormone concentration versus time-dependent change". eng. In: *Psychoneuroendocrinology* 28.7 (Oct. 2003), pp. 916–931. ISSN: 0306-4530. DOI: 10.1016/s0306-4530(02)00108-7.

[Ram15] Alexander Rampp, Jens Barth, Samuel Schülein, Karl-Günter Gaßmann, Jochen Klucken, and Björn M. Eskofier. "Inertial Sensor-Based Stride Parameter Calculation From Gait Sequences in Geriatric Patients". In: *IEEE Transactions on Biomedical Engineering* 62.4 (Apr. 2015). Conference Name: IEEE Transactions on Biomedical Engineering, pp. 1089–1097. ISSN: 1558-2531. DOI: 10.1109/TBME.2014.2368211.

[Ric21a] Robert Richer, Arne Kuderle, Jana Dorr, Nicolas Rohleder, and Bjoern M. Eskofier. "Assessing the Influence of the Inner Clock on the Cortisol Awakening Response and Pre-Awakening Movement". en. In: *2021 IEEE EMBS International Conference on Biomedical and Health Informatics (BHI)*. Athens, Greece: IEEE, July 2021, pp. 1–4. ISBN: 978-1-66540-358-0. DOI: 10.1109/BHI50953.2021.9508529. URL: https://ieeexplore.ieee.org/document/9508529/ (visited on 04/19/2022).

[Ric21b] Robert Richer, Arne Küderle, Martin Ullrich, Nicolas Rohleder, and Bjoern M. Eskofier. "BioPsyKit: A Python package for the analysis of biopsychological data". en. In: *Journal of Open Source Software* 6.66 (Oct. 2021), p. 3702. ISSN: 2475-9066. DOI: 10.21105/joss.03702. URL: https://joss.theoj.org/papers/10.21105/joss.03702 (visited on 04/22/2022).

[Ric22] Robert Richer, V. Koch, Arne Küderle, Victoria Müller, Vanessa Wirth, Marc Stamminger, Nicolas Rohleder, and Björn Eskofier. "Detection of Acute Psychosocial Stress from Body Movements using Machine Learning". In: 2022.

[Roe10] Karin Roelofs, Muriel A. Hagenaars, and John Stins. "Facing Freeze: Social Threat Induces Bodily Freeze in Humans". en. In: *Psychol Sci* 21.11 (Nov. 2010). tex.ids: Roelofs2010, pp. 1575–1581. ISSN: 0956-7976, 1467-9280. DOI: 10.1177/0956797610384746. URL: 10.1177/0956797610384746 (visited on 10/18/2020).

[Roe17] Karin Roelofs. "Freeze for action: neurobiological mechanisms in animal and human freezing". In: *Philosophical Transactions of the Royal Society B: Biological Sciences* 372.1718 (Apr. 2017). Publisher: Royal Society, p. 20160206. DOI: 10.1098/rstb.2016.0206. URL: https://royalsocietypublishing.org/doi/10.1098/rstb.2016.0206 (visited on 04/26/2022).

[Roh19] Nicolas Rohleder. "Stress and inflammation - The need to address the gap in the transition between acute and chronic stress effects". eng. In: *Psychoneuroen-*

docrinology 105 (July 2019), pp. 164–171. ISSN: 1873-3360. DOI: 10.1016/j.psyneuen.2019.02.021.

[Sar19] Georgia Sarolidou, John Axelsson, Tina Sundelin, Julie Lasselin, Christina Regenbogen, Kimmo Sorjonen, Johan N. Lundström, Mats Lekander, and Mats J. Olsson. "Emotional expressions of the sick face". en. In: *Brain, Behavior, and Immunity* 80 (Aug. 2019), pp. 286–291. ISSN: 0889-1591. DOI: 10.1016/j.bbi.2019.04.003. URL: https://www.sciencedirect.com/science/article/pii/S0889159118311656 (visited on 05/20/2022).

[Sla15] Danica C. Slavish, Jennifer E. Graham-Engeland, Joshua M. Smyth, and Christopher G. Engeland. "Salivary markers of inflammation in response to acute stress". en. In: *Brain, Behavior, and Immunity* 44 (Feb. 2015), pp. 253–269. ISSN: 0889-1591. DOI: 10.1016/j.bbi.2014.08.008. URL: https://www.sciencedirect.com/science/article/pii/S0889159114004255 (visited on 01/12/2022).

[Ste01] Andrew Steptoe, Gonneke Willemsen, Natalie Owen, Louise Flower, and Vidya Mohamed-Ali. "Acute mental stress elicits delayed increases in circulating inflammatory cytokine levels". In: *Clinical Science* 101.2 (July 2001), pp. 185–192. ISSN: 0143-5221. DOI: 10.1042/cs1010185. URL: https://doi.org/10.1042/cs1010185 (visited on 05/19/2022).

[Str11] David L. Streiner and Geoffrey R. Norman. "Correction for Multiple Testing: Is There a Resolution?" en. In: *Chest* 140.1 (July 2011), pp. 16–18. ISSN: 0012-3692. DOI: 10.1378/chest.11-0523. URL: https://www.sciencedirect.com/science/article/pii/S0012369211603401 (visited on 05/15/2022).

[Ulr09] Yvonne M. Ulrich-Lai and James P. Herman. "Neural regulation of endocrine and autonomic stress responses". en. In: *Nat Rev Neurosci* 10.6 (June 2009). Bandiera_abtest: a Cg_type: Nature Research Journals Number: 6 Primary_atype: Reviews Publisher: Nature Publishing Group, pp. 397–409. ISSN: 1471-0048. DOI: 10.1038/nrn2647. URL: https://www.nature.com/articles/nrn2647 (visited on 01/04/2022).

[Val18] Raphael Vallat. "Pingouin: statistics in Python". en. In: *Journal of Open Source Software* 3.31 (Nov. 2018), p. 1026. ISSN: 2475-9066. DOI: 10.21105/joss.01026. URL: https://joss.theoj.org/papers/10.21105/joss.01026 (visited on 05/03/2022).

[Wat88] David Watson, Lee Anna Clark, and Auke Tellegen. "Development and validation of brief measures of positive and negative affect: The PANAS scales". In: *Journal of Personality and Social Psychology* 54.6 (1988). Place: US Publisher: American

Psychological Association, pp. 1063–1070. ISSN: 1939-1315. DOI: 10.1037/0022-3514.54.6.1063.

[Wie13] Uta S. Wiemers, Daniela Schoofs, and Oliver T. Wolf. "A friendly version of the Trier Social Stress Test does not activate the HPA axis in healthy men and women". en. In: *Stress* 16.2 (Mar. 2013), pp. 254–260. ISSN: 1025-3890, 1607-8888. DOI: 10.3109/10253890.2012.714427. URL: 10.3109/10253890.2012.714427 (visited on 10/17/2020).

[Xse21] Xsens. *MVN User Manual*. en. Apr. 2021. URL: https://www.xsens.com/hubfs/Downloads/usermanual/MVN_User_Manual.pdf (visited on 04/19/2022).

[Zän20] Sandra Zänkert, Brigitte M. Kudielka, and Stefan Wüst. "Effect of sugar administration on cortisol responses to acute psychosocial stress". en. In: *Psychoneuroendocrinology* 115 (May 2020), p. 104607. ISSN: 0306-4530. DOI: 10.1016/j.psyneuen.2020.104607. URL: https://www.sciencedirect.com/science/article/pii/S0306453020300263 (visited on 04/13/2022).

[Zee19] Sophie van der Zee, Ronald Poppe, Paul J Taylor, and Ross Anderson. "To freeze or not to freeze: A culture-sensitive motion capture approach to detecting deceit". In: *PLoS One* 14.4 (Apr. 2019), e0215000. ISSN: 1932-6203. DOI: 10.1371/journal.pone.0215000. URL: http://dx.doi.org/10.1371/journal.pone.0215000.

[Zen08] JA Zeni, JG Richards, and J.S. Higginson. "Two simple methods for determining gait events during treadmill and overground walking using kinematic data". In: *Gait Posture* 27.4 (May 2008), pp. 710–714. ISSN: 0966-6362. DOI: 10.1016/j.gaitpost.2007.07.007. URL: https://www.ncbi.nlm.nih.gov/pmc/articles/PMC2384115/ (visited on 03/30/2022).

Appendix A

Additional Figures

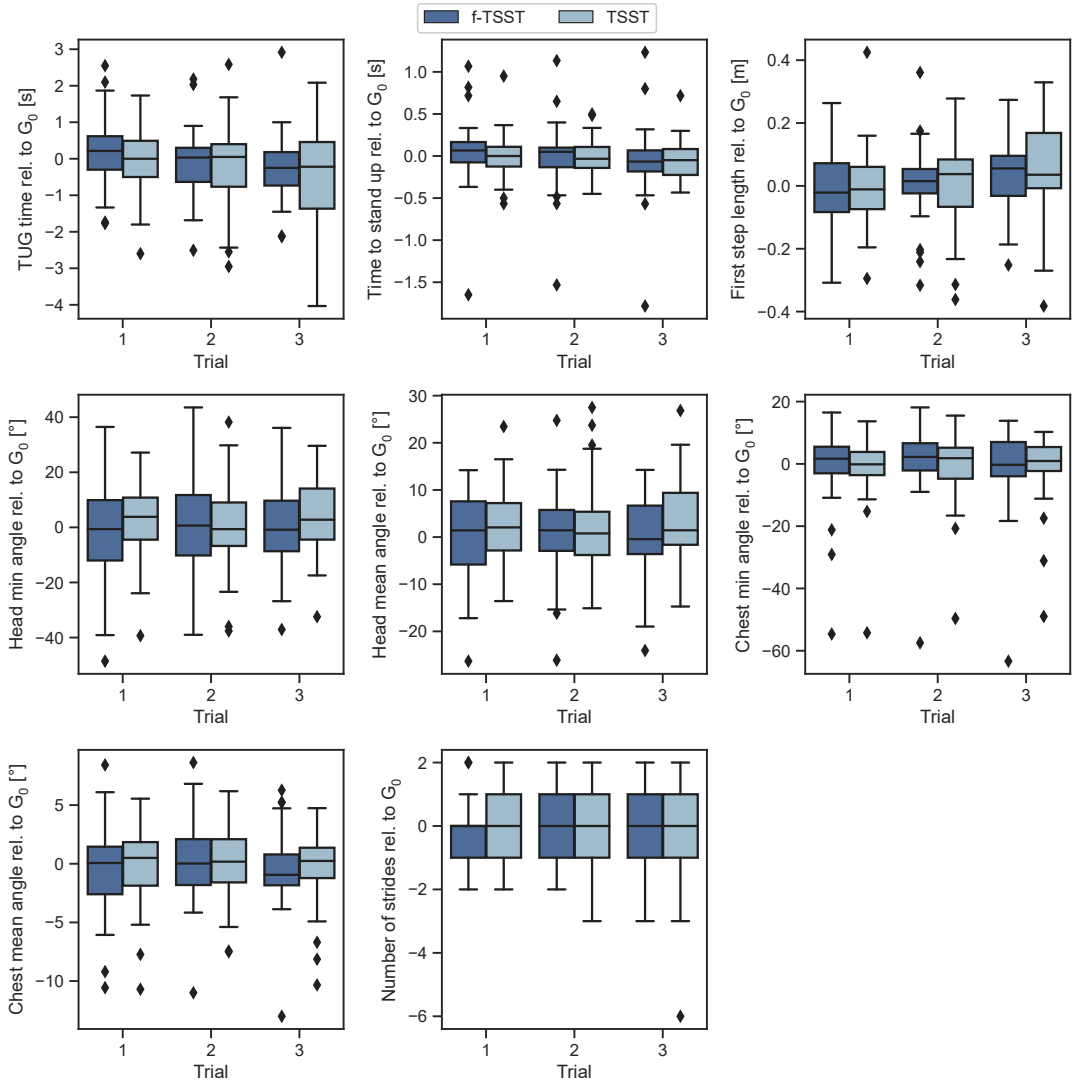

Figure A.1: TUG features relative to baseline (G_0)

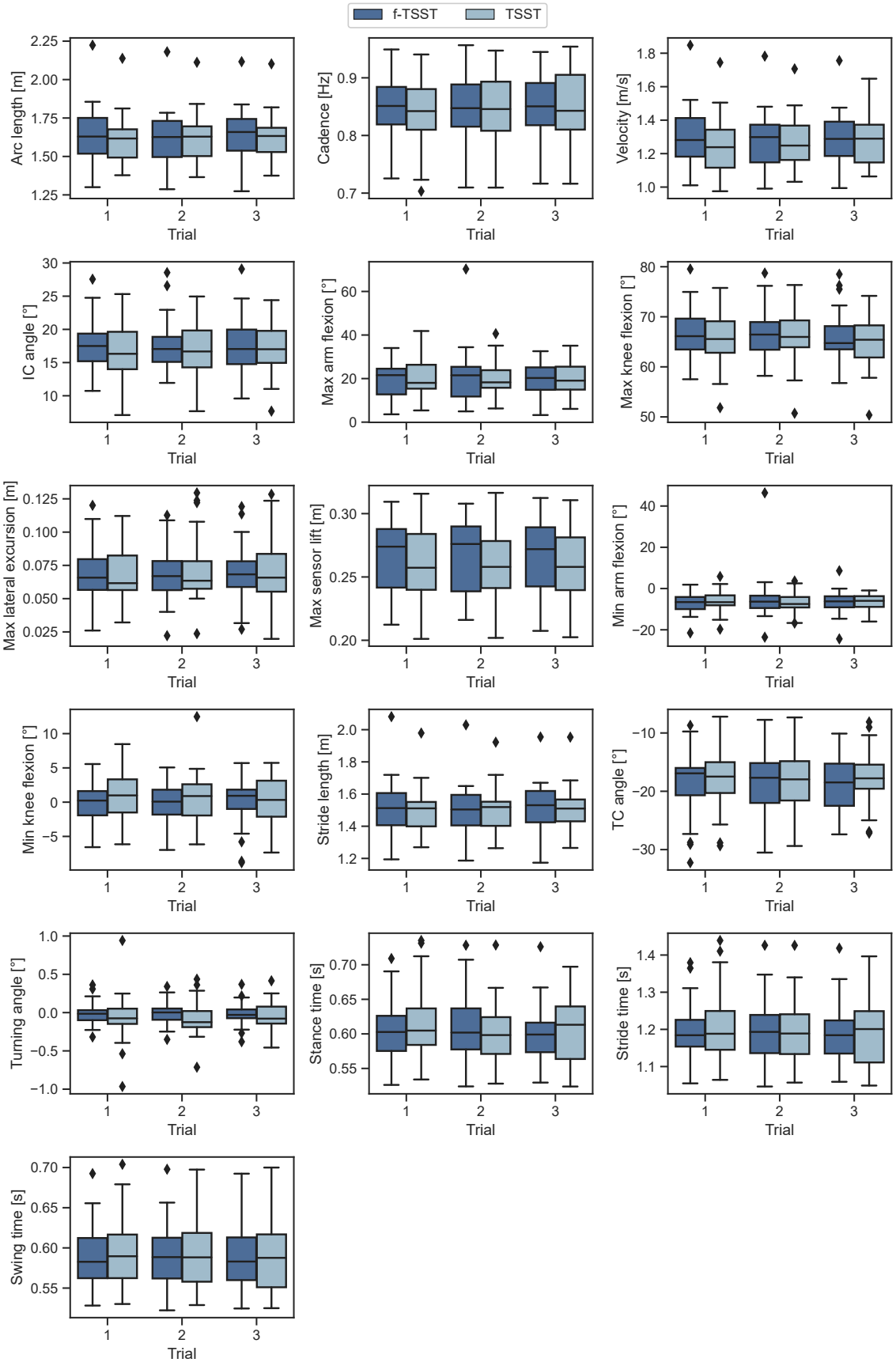

Figure A.2: Cadence-matched spatiotemporal features

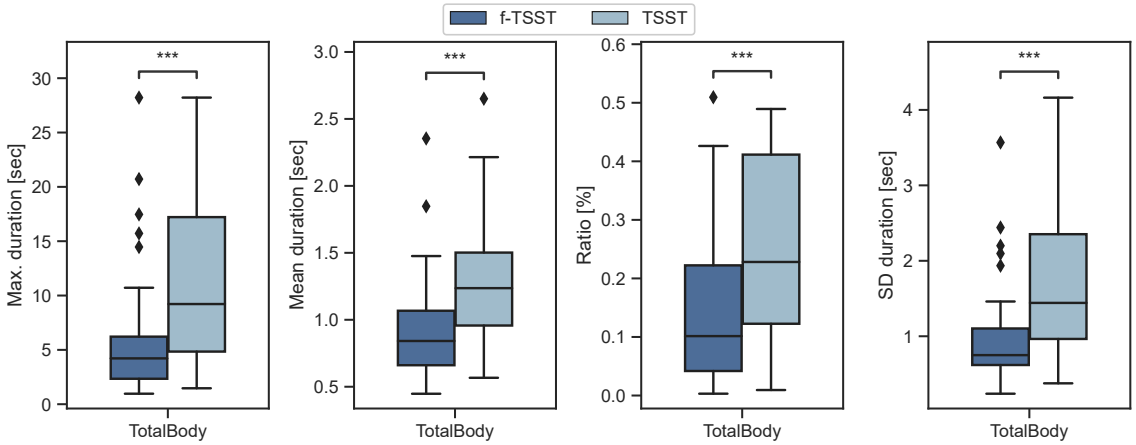

Figure A.3: Total body *static periods* feature (gyr channel)

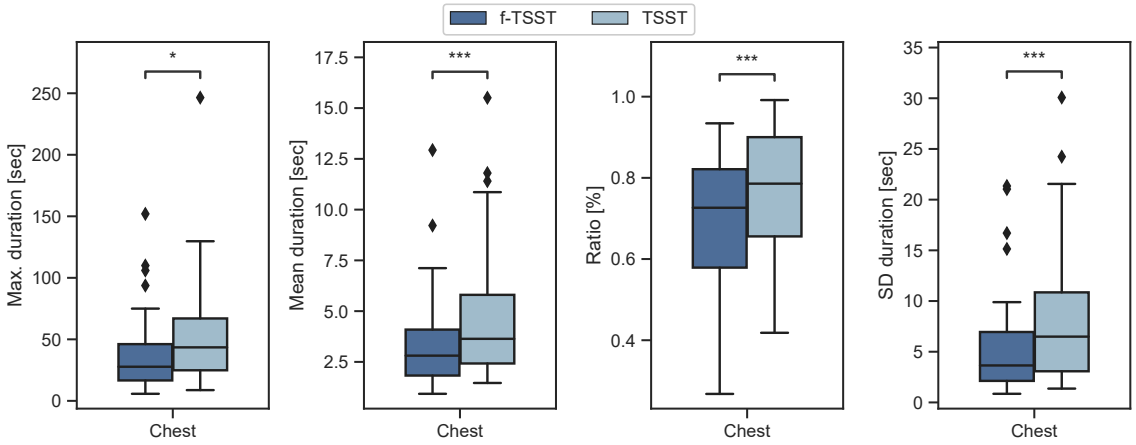

Figure A.4: Chest *static periods* feature (gyr channel)

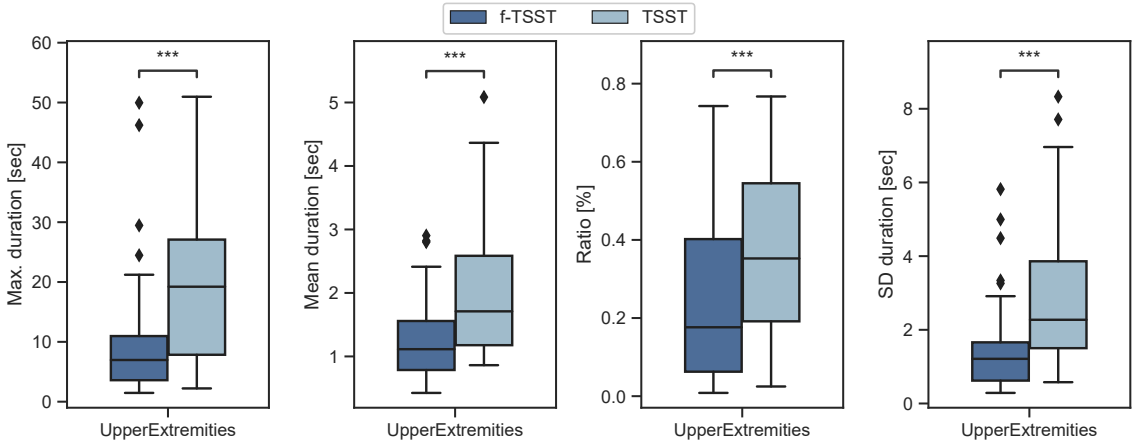

Figure A.5: Upper extremities *static periods* feature (gyr channel)

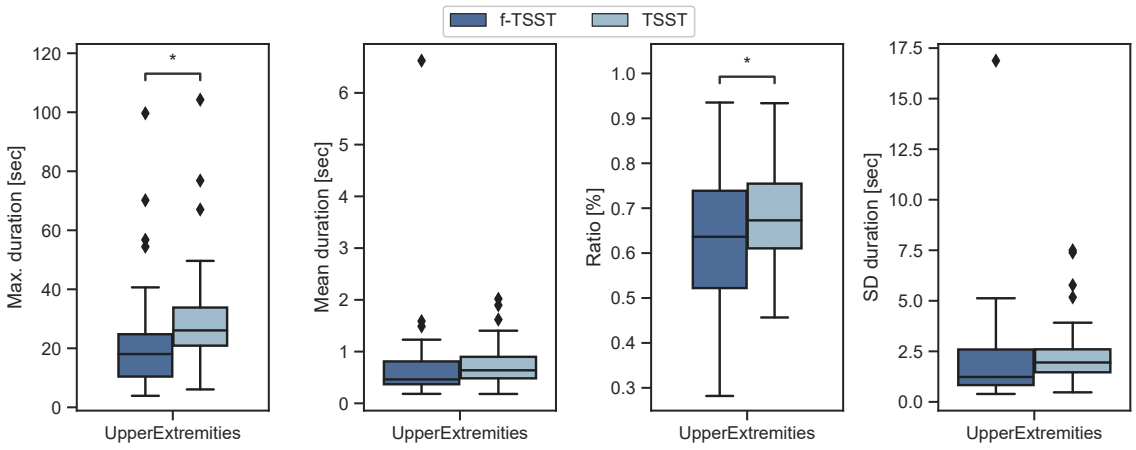

Figure A.6: Upper extremities *below threshold* feature (gyr channel)

Appendix B

Additional Tables

Table B.1: Recorded channels as described in Xsens documentation [Xse21]

Type	Channel	Description
Segment	ori	1×4 quaternion vector (q_0, q_1, q_2, q_3) describing the orientation of the segment with respect to the global frame
	pos	1×3 position vector (x, y, z) of the origin of the segment in the global frame in m
	vel	1×3 velocity vector (x, y, z) of the origin of the segment in the global frame in $\mathrm{m\,s^{-1}}$
	acc	1×3 acceleration vector (x, y, z) of the origin of the segment in the global frame in $\mathrm{m\,s^{-2}}$
	gyr	1×3 angular velocity vector (x, y, z) of the segment in the global frame in $\mathrm{rad\,s^{-1}}$
	ang_acc	1×3 angular acceleration vector (x, y, z) of the segment in the global frame in $\mathrm{rad\,s^{-2}}$
Sensor	acc	1×3 sensor acceleration vector (x, y, z) in $\mathrm{m\,s^{-2}}$
	mag	1×3 sensor magnetic field vector (x, y, z) of the sensor in a.u.
	ori	1×4 sensor orientation quaternion vector (q_0, q_1, q_2, q_3) of the sensor in the global frame
Joint	ang	1×3 Euler representation of the joint angle vector (x, y, z) in deg, calculated using the Euler sequence ZXY using the ISB based coordinate system.
Center of Mass	pos	1×3 position vector (x, y, z) of the center of mass in the global frame in m
Foot Contacts	foot_contacts	1×4 binary vector indicating foot floor contacts $(\mathrm{LeftToe}, \mathrm{LeftHeel}, \mathrm{RightToe}, \mathrm{RightHeel})$

Table B.2: t-test results of generic features

Body part	Channel	Metric	$t(38)$	p	Hedges' g
CenterMass	acc	cov	0.210	0.835	0.048
		mean	−0.649	0.520	−0.118
		sd	0.727	0.472	0.164
	vel	cov	−0.875	0.387	−0.192
		mean	−1.343	0.187	−0.154
		sd	−1.161	0.253	−0.252
Head	acc	abs_energy	0.953	0.347	0.212
		cov	1.156	0.255	0.253
		entropy	−2.052	0.047 *	−0.278
		fft_aggregated_centroid	1.654	0.106	0.237
		fft_aggregated_kurtosis	−0.467	0.643	−0.098
		fft_aggregated_skew	−2.132	0.039 *	−0.309
		fft_aggregated_variance	1.919	0.063	0.276
		max_val	0.899	0.374	0.201
		mean	−4.497	<0.001***	−0.465
		mean_crossing	1.865	0.070	0.177
		sd	0.594	0.556	0.125
	gyr	abs_energy	−1.640	0.109	−0.212
		cov	5.408	<0.001***	0.682
		entropy	−7.064	<0.001***	−0.667
		fft_aggregated_centroid	−1.207	0.235	−0.245
		fft_aggregated_kurtosis	1.943	0.059	0.294
		fft_aggregated_skew	1.806	0.079	0.284
		fft_aggregated_variance	−1.215	0.232	−0.257
		max_val	0.665	0.510	0.146
		mean	−5.601	<0.001***	−0.467
		mean_crossing	−4.495	<0.001***	−0.586
		sd	−1.515	0.138	−0.187
	vel	abs_energy	−1.137	0.263	−0.254
		cov	−0.913	0.367	−0.204
		entropy	0.624	0.537	0.122
		fft_aggregated_centroid	2.104	0.042 *	0.305

		fft_aggregated_kurtosis	−1.948	0.059	−0.340
		fft_aggregated_skew	−2.193	0.034 *	−0.322
		fft_aggregated_variance	2.431	0.020 *	0.380
		max_val	−1.097	0.279	−0.247
		mean	−2.528	0.016 *	−0.278
		mean_crossing	2.667	0.011 *	0.344
		sd	−1.385	0.174	−0.297
LeftHand	acc	abs_energy	−1.348	0.186	−0.167
		cov	2.949	0.005 **	0.487
		entropy	−2.999	0.005 **	−0.403
		fft_aggregated_centroid	0.302	0.764	0.052
		fft_aggregated_kurtosis	−0.940	0.353	−0.192
		fft_aggregated_skew	−0.597	0.554	−0.118
		fft_aggregated_variance	1.156	0.255	0.194
		max_val	−0.212	0.833	−0.035
		mean	−2.402	0.021 *	−0.293
		mean_crossing	0.186	0.854	0.025
		sd	−1.015	0.317	−0.129
	gyr	abs_energy	−1.900	0.065	−0.254
		cov	2.840	0.007 **	0.522
		entropy	−3.153	0.003 **	−0.479
		fft_aggregated_centroid	−0.067	0.947	−0.011
		fft_aggregated_kurtosis	−1.689	0.099	−0.292
		fft_aggregated_skew	−0.636	0.529	−0.110
		fft_aggregated_variance	0.909	0.369	0.139
		max_val	−1.490	0.145	−0.199
		mean	−2.802	0.008 **	−0.347
		mean_crossing	−0.872	0.389	−0.126
		sd	−1.731	0.092	−0.212
	vel	abs_energy	−1.899	0.065	−0.402
		cov	0.532	0.598	0.098
		entropy	−1.989	0.054	−0.234
		fft_aggregated_centroid	2.593	0.013 *	0.517
		fft_aggregated_kurtosis	−2.595	0.013 *	−0.545
		fft_aggregated_skew	−2.705	0.010 *	−0.541
		fft_aggregated_variance	2.999	0.005 **	0.616

		max_val	−0.989	0.329	−0.224
		mean	−2.902	0.006 **	−0.417
		mean_crossing	−0.856	0.397	−0.118
		sd	−2.063	0.046 *	−0.373
LowerExtremities	acc	cov	−0.933	0.357	−0.206
		max_val	−0.182	0.856	−0.041
		mean	−0.340	0.736	−0.069
		sd	−0.175	0.862	−0.040
	gyr	cov	−1.015	0.316	−0.177
		max_val	−1.484	0.146	−0.303
		mean	−1.150	0.257	−0.132
		sd	−1.257	0.216	−0.177
	vel	cov	−0.824	0.415	−0.172
		max_val	−1.020	0.314	−0.229
		mean	−1.546	0.130	−0.192
		sd	−1.065	0.294	−0.239
RightHand	acc	abs_energy	−1.539	0.132	−0.257
		cov	0.688	0.496	0.110
		entropy	−0.128	0.898	−0.020
		fft_aggregated_centroid	1.210	0.234	0.172
		fft_aggregated_kurtosis	−0.387	0.701	−0.072
		fft_aggregated_skew	−1.682	0.101	−0.262
		fft_aggregated_variance	1.031	0.309	0.155
		max_val	−1.134	0.264	−0.208
		mean	−1.665	0.104	−0.229
		mean_crossing	1.545	0.131	0.259
		sd	−1.638	0.110	−0.244
	gyr	abs_energy	−1.800	0.080	−0.312
		cov	1.815	0.077	0.319
		entropy	−1.422	0.163	−0.228
		fft_aggregated_centroid	0.298	0.767	0.045
		fft_aggregated_kurtosis	−1.688	0.100	−0.276
		fft_aggregated_skew	−1.148	0.258	−0.175
		fft_aggregated_variance	0.649	0.520	0.100
		max_val	−1.859	0.071	−0.279
		mean	−1.823	0.076	−0.268

		mean_crossing	0.578	0.567	0.092
		sd	−2.002	0.052	−0.283
	vel	abs_energy	−1.780	0.083	−0.357
		cov	0.374	0.710	0.071
		entropy	−0.561	0.578	−0.077
		fft_aggregated_centroid	1.827	0.076	0.383
		fft_aggregated_kurtosis	−1.100	0.278	−0.225
		fft_aggregated_skew	−1.484	0.146	−0.311
		fft_aggregated_variance	1.606	0.116	0.336
		max_val	−0.900	0.374	−0.197
		mean	−2.218	0.033 *	−0.323
		mean_crossing	1.116	0.271	0.172
		sd	−2.318	0.026 *	−0.362
Chest	acc	abs_energy	−1.158	0.254	−0.141
		cov	1.109	0.274	0.177
		entropy	−1.231	0.226	−0.155
		fft_aggregated_centroid	2.311	0.026 *	0.323
		fft_aggregated_kurtosis	2.422	0.020 *	0.287
		fft_aggregated_skew	−2.202	0.034 *	−0.309
		fft_aggregated_variance	0.819	0.418	0.151
		max_val	0.530	0.599	0.103
		mean	−1.580	0.122	−0.186
		mean_crossing	0.867	0.392	0.102
		sd	−0.736	0.466	−0.088
	gyr	abs_energy	−2.349	0.024 *	−0.273
		cov	1.244	0.221	0.158
		entropy	−2.038	0.049 *	−0.255
		fft_aggregated_centroid	2.021	0.050	0.283
		fft_aggregated_kurtosis	−2.062	0.046 *	−0.276
		fft_aggregated_skew	−2.322	0.026 *	−0.334
		fft_aggregated_variance	1.841	0.073	0.237
		max_val	−0.898	0.375	−0.141
		mean	−3.585	<0.001***	−0.374
		mean_crossing	2.221	0.032 *	0.294
		sd	−2.139	0.039 *	−0.256

	vel	abs_energy	−1.091	0.282		−0.244
		cov	−0.841	0.406		−0.185
		entropy	0.414	0.681		0.080
		fft_aggregated_centroid	0.886	0.381		0.130
		fft_aggregated_kurtosis	−1.010	0.319		−0.149
		fft_aggregated_skew	−0.902	0.373		−0.126
		fft_aggregated_variance	1.624	0.113		0.243
		max_val	−1.059	0.296		−0.238
		mean	−1.656	0.106		−0.183
		mean_crossing	1.244	0.221		0.156
		sd	−1.209	0.234		−0.258
TotalBody	acc	abs_energy	0.255	0.800		0.058
		cov	−0.627	0.534		−0.133
		fft_aggregated_centroid	2.309	0.026	*	0.241
		fft_aggregated_kurtosis	1.229	0.226		0.138
		fft_aggregated_skew	−3.022	0.004	**	−0.332
		fft_aggregated_variance	1.553	0.129		0.228
		max_val	−0.176	0.861		−0.040
		mean	−2.013	0.051		−0.278
		sd	−0.196	0.846		−0.045
	gyr	abs_energy	−2.496	0.017	*	−0.372
		cov	0.265	0.792		0.038
		fft_aggregated_centroid	2.073	0.045	*	0.255
		fft_aggregated_kurtosis	−1.885	0.067		−0.294
		fft_aggregated_skew	−2.425	0.020	*	−0.322
		fft_aggregated_variance	2.148	0.038	*	0.268
		max_val	−1.925	0.062		−0.325
		mean	−3.103	0.004	**	−0.382
		sd	−2.288	0.028	*	−0.301
	vel	abs_energy	−1.021	0.314		−0.229
		cov	−0.739	0.464		−0.158
		fft_aggregated_centroid	1.780	0.083		0.296
		fft_aggregated_kurtosis	−1.633	0.111		−0.274
		fft_aggregated_skew	−1.775	0.084		−0.283
		fft_aggregated_variance	2.302	0.027	*	0.369
		max_val	−1.010	0.319		−0.227

		mean	−2.324	0.026 *	−0.277
		sd	−1.234	0.225	−0.271
Trunk	acc	abs_energy	0.659	0.514	0.145
		cov	0.566	0.575	0.093
		fft_aggregated_centroid	2.369	0.023 *	0.316
		fft_aggregated_kurtosis	2.131	0.040 *	0.241
		fft_aggregated_skew	−2.727	0.010 **	−0.360
		fft_aggregated_variance	1.385	0.174	0.239
		max_val	0.768	0.447	0.171
		mean	−1.956	0.058	−0.241
		sd	−0.368	0.715	−0.064
	gyr	abs_energy	−2.010	0.052	−0.257
		cov	1.119	0.270	0.145
		fft_aggregated_centroid	1.571	0.124	0.235
		fft_aggregated_kurtosis	−1.802	0.080	−0.262
		fft_aggregated_skew	−1.876	0.068	−0.285
		fft_aggregated_variance	1.500	0.142	0.216
		max_val	−0.738	0.465	−0.137
		mean	−3.579	<0.001***	−0.374
		sd	−1.892	0.066	−0.252
	vel	abs_energy	−1.084	0.285	−0.243
		cov	−0.836	0.408	−0.183
		fft_aggregated_centroid	0.217	0.829	0.035
		fft_aggregated_kurtosis	−0.307	0.761	−0.052
		fft_aggregated_skew	−0.214	0.832	−0.034
		fft_aggregated_variance	0.906	0.370	0.145
		max_val	−1.062	0.295	−0.239
		mean	−1.628	0.112	−0.182
		sd	−1.213	0.233	−0.260

UpperExtremities	acc	abs_energy	−1.622	0.113	−0.231
		cov	1.707	0.096	0.245
		max_val	−1.146	0.259	−0.185
		mean	−2.407	0.021 *	−0.294
		sd	−1.675	0.102	−0.221
	gyr	abs_energy	−2.309	0.026 *	−0.350
		cov	2.918	0.006 **	0.438
		max_val	−1.943	0.059	−0.261
		mean	−2.897	0.006 **	−0.371
		sd	−2.173	0.036 *	−0.290
	vel	abs_energy	−1.415	0.165	−0.311
		cov	−0.298	0.767	−0.064
		max_val	−0.905	0.371	−0.203
		mean	−2.780	0.008 **	−0.351
		sd	−1.717	0.094	−0.346
jC1Head	ang	cov	2.101	0.042 *	0.346
		entropy	−2.058	0.046 *	−0.384
		fft_aggregated_centroid	0.891	0.379	0.176
		fft_aggregated_kurtosis	−0.573	0.570	−0.115
		fft_aggregated_skew	−0.367	0.716	−0.076
		fft_aggregated_variance	1.387	0.174	0.312
		max_val	−1.067	0.293	−0.150
		mean	−3.142	0.003 **	−0.538
		sd	−0.097	0.923	−0.013
jLeftElbow	ang	cov	−0.561	0.578	−0.109
		fft_aggregated_centroid	−0.245	0.808	−0.041
		fft_aggregated_kurtosis	−0.633	0.530	−0.092
		fft_aggregated_skew	−0.132	0.896	−0.019
		fft_aggregated_variance	1.280	0.208	0.221
		max_val	0.097	0.924	0.019
		mean	1.468	0.150	0.257
		sd	−0.477	0.636	−0.097

jLeftKnee	ang	cov	−0.888	0.380	−0.151
		max_val	−0.427	0.672	−0.067
		mean	1.000	0.324	0.123
		sd	−0.830	0.412	−0.095
jRightElbow	ang	cov	0.056	0.956	0.010
		fft_aggregated_centroid	−0.145	0.885	−0.022
		fft_aggregated_kurtosis	−0.724	0.474	−0.117
		fft_aggregated_skew	−0.365	0.717	−0.054
		fft_aggregated_variance	0.852	0.399	0.142
		max_val	0.688	0.496	0.126
		mean	1.268	0.212	0.224
		sd	−0.071	0.944	−0.014
jRightKnee	ang	cov	−0.324	0.747	−0.042
		max_val	−1.706	0.096	−0.324
		mean	−1.125	0.267	−0.243
		sd	−1.316	0.196	−0.133

Table B.3: t-test results of euclidean distance features

Body part	Channel	Metric	$t(38)$	p	Hedges' g
LeftFoot_RightFoot	pos	mean	1.413	0.166	0.209
		sd	−1.108	0.275	−0.183
LeftHand_Head	pos	mean	−1.398	0.170	−0.180
		sd	−1.199	0.238	−0.180
LeftHand_RightHand	pos	mean	−1.928	0.061	−0.298
		sd	1.076	0.289	0.189
RightHand_Head	pos	mean	−1.366	0.180	−0.157
		sd	−0.646	0.522	−0.095

Table B.4: t-test results of static period features

Body part	Channel	Metric	$t(38)$	p	Hedges' g
Head	gyr	count_per_min	−0.338	0.737	−0.043
		max_duration_sec	3.754	<0.001***	0.745
		mean_duration_sec	5.405	<0.001***	0.854
		ratio_percent	6.874	<0.001***	0.685
		sd_duration_sec	4.323	<0.001***	0.810
	vel	count_per_min	−2.398	0.022 *	−0.341
		max_duration_sec	2.183	0.035 *	0.433
		mean_duration_sec	2.469	0.018 *	0.295
		ratio_percent	4.222	<0.001***	0.404
		sd_duration_sec	2.311	0.026 *	0.391
LeftHand_RightHand	gyr	count_per_min	0.815	0.420	0.124
		max_duration_sec	3.447	0.001 **	0.478
		mean_duration_sec	5.446	<0.001***	0.839
		ratio_percent	6.621	<0.001***	0.591
		sd_duration_sec	4.780	<0.001***	0.638
	vel	count_per_min	0.229	0.820	0.041
		max_duration_sec	3.754	<0.001***	0.670
		mean_duration_sec	3.534	0.001 **	0.550
		ratio_percent	4.556	<0.001***	0.524
		sd_duration_sec	3.795	<0.001***	0.630
LowerExtremities	gyr	count_per_min	−3.204	0.003 **	−0.374
		max_duration_sec	1.873	0.069	0.244
		mean_duration_sec	2.067	0.046 *	0.209
		ratio_percent	2.530	0.016 *	0.230
		sd_duration_sec	2.084	0.044 *	0.250
	vel	count_per_min	−2.747	0.009 **	−0.340
		max_duration_sec	1.601	0.118	0.147
		mean_duration_sec	2.253	0.030 *	0.165
		ratio_percent	2.455	0.019 *	0.217
		sd_duration_sec	2.698	0.010 *	0.183
Chest	gyr	count_per_min	−5.377	<0.001***	−0.602
		max_duration_sec	2.234	0.031 *	0.392

		mean_duration_sec	3.859	<0.001***	0.533
		ratio_percent	4.942	<0.001***	0.475
		sd_duration_sec	3.573	<0.001***	0.516
	vel	count_per_min	−1.908	0.064	−0.253
		max_duration_sec	1.683	0.101	0.208
		mean_duration_sec	1.549	0.130	0.196
		ratio_percent	2.504	0.017 *	0.257
		sd_duration_sec	2.136	0.039 *	0.238
TotalBody	gyr	count_per_min	4.691	<0.001***	0.455
		max_duration_sec	4.178	<0.001***	0.738
		mean_duration_sec	6.483	<0.001***	0.895
		ratio_percent	6.591	<0.001***	0.712
		sd_duration_sec	5.332	<0.001***	0.822
	vel	count_per_min	0.538	0.594	0.082
		max_duration_sec	4.867	<0.001***	0.864
		mean_duration_sec	4.760	<0.001***	0.664
		ratio_percent	5.322	<0.001***	0.504
		sd_duration_sec	5.308	<0.001***	0.836
Trunk	gyr	count_per_min	−3.973	<0.001***	−0.608
		max_duration_sec	5.201	<0.001***	0.808
		mean_duration_sec	4.519	<0.001***	0.686
		ratio_percent	6.306	<0.001***	0.556
		sd_duration_sec	4.889	<0.001***	0.757
	vel	count_per_min	−2.744	0.009 **	−0.401
		max_duration_sec	2.160	0.037 *	0.409
		mean_duration_sec	2.133	0.039 *	0.269
		ratio_percent	3.286	0.002 **	0.330
		sd_duration_sec	2.404	0.021 *	0.382

UpperExtremities	gyr	count_per_min	1.791	0.081	0.240
		max_duration_sec	4.920	<0.001***	0.757
		mean_duration_sec	5.289	<0.001***	0.837
		ratio_percent	7.005	<0.001***	0.625
		sd_duration_sec	4.900	<0.001***	0.814
	vel	count_per_min	0.614	0.543	0.107
		max_duration_sec	4.204	<0.001***	0.799
		mean_duration_sec	3.698	<0.001***	0.586
		ratio_percent	5.321	<0.001***	0.556
		sd_duration_sec	4.264	<0.001***	0.723

Table B.5: t-test results of below threshold features

Body part	Channel	Metric	$t(38)$	p	Hedges' g
Head	gyr	count_per_min	−3.813	<0.001***	−0.547
		max_duration_sec	1.273	0.211	0.272
		mean_duration_sec	1.032	0.309	0.232
		ratio_percent	3.485	0.001 **	0.488
		sd_duration_sec	1.129	0.266	0.253
LeftHand_RightHand	gyr	count_per_min	−2.540	0.015 *	−0.249
		max_duration_sec	2.410	0.021 *	0.455
		mean_duration_sec	1.701	0.097	0.335
		ratio_percent	3.293	0.002 **	0.396
		sd_duration_sec	1.887	0.067	0.371
LowerExtremities	gyr	count_per_min	0.015	0.988	0.002
		max_duration_sec	−0.538	0.594	−0.111
		mean_duration_sec	−0.966	0.340	−0.186
		ratio_percent	0.311	0.757	0.054
		sd_duration_sec	−0.734	0.468	−0.128
T8	gyr	count_per_min	−0.208	0.837	−0.025
		max_duration_sec	1.173	0.248	0.234
		mean_duration_sec	−0.689	0.495	−0.131
		ratio_percent	1.735	0.091	0.239
		sd_duration_sec	0.144	0.887	0.027
TotalBody	gyr	count_per_min	2.087	0.044 *	0.271
		max_duration_sec	0.976	0.335	0.190
		mean_duration_sec	0.533	0.597	0.064
		ratio_percent	1.564	0.126	0.250
		sd_duration_sec	0.877	0.386	0.136
Trunk	gyr	count_per_min	−0.191	0.849	−0.024
		max_duration_sec	0.943	0.352	0.169
		mean_duration_sec	−0.691	0.494	−0.114
		ratio_percent	2.803	0.008 **	0.342
		sd_duration_sec	−0.166	0.869	−0.027

UpperExtremities	gyr	count_per_min	–0.312	0.756	–0.057
		max_duration_sec	2.109	0.042 *	0.400
		mean_duration_sec	–0.160	0.874	–0.027
		ratio_percent	2.433	0.020 *	0.404
		sd_duration_sec	0.794	0.432	0.140

Table B.6: Gender differences for (f-)TSST motion features; only significant features are shown

Body part	Channel	Type	Metric	t	p	Hedges' g
LeftHand_Head	pos	euclidean_distance	mean	2.320	0.026*	0.729
LowerExtremities	gyr	below_threshold	count_per_min	2.195	0.038*	0.646
			ratio_percent	–2.573	0.016*	–0.766
RightHand_Head	pos	euclidean_distance	mean	2.849	0.007**	0.894
TotalBody	gyr	max_val	max_val	–2.079	0.048*	–0.686
jC1Head	ang	entropy	entropy	–2.107	0.042*	–0.643
jRightElbow	ang	cov	cov	–2.771	0.009**	–0.892

Table B.7: Results of linear regression predicting PASA-Challenge with upper extremities features; β: standardized regression coefficient; σ: standard error; adj.: adjusted

components	β	σ	t	p	R^2	adj. R^2
UpperExtremities_PCA_2	0.073	0.054	1.366	0.181	0.223	0.156
UpperExtremities_PCA_3	-0.146	0.067	-2.175	0.036	0.223	0.156
UpperExtremities_PCA_5	-0.162	0.087	-1.853	0.072	0.223	0.156

Table B.8: Results of linear regression predicting PANAS-NegativeAffect with head features; β: standardized regression coefficient; σ: standard error; adj.: adjusted

components	β	σ	t	p	R^2	adj. R^2
Head_PCA_2	0.116	0.049	2.340	0.025	0.173	0.127
Head_PCA_6	-0.117	0.082	-1.427	0.162	0.173	0.127

Table B.9: Results of linear regression predicting PANAS-PositiveAffect with chest features; β: standardized regression coefficient; σ: standard error; adj.: adjusted

components	β	σ	t	p	R^2	adj. R^2
Chest_PCA_3	0.227	0.082	2.773	0.009	0.232	0.166
Chest_PCA_5	-0.119	0.112	-1.061	0.296	0.232	0.166
Chest_PCA_7	0.181	0.136	1.326	0.194	0.232	0.166

Table B.10: Results of linear regression predicting PASA-Threat with chest features; β: standardized regression coefficient; σ: standard error; adj.: adjusted

components	β	σ	t	p	R^2	adj. R^2
Chest_PCA_1	0.106	0.032	3.277	0.002	0.396	0.305
Chest_PCA_4	0.066	0.055	1.199	0.239	0.396	0.305
Chest_PCA_5	0.065	0.065	1.011	0.320	0.396	0.305
Chest_PCA_6	0.126	0.075	1.675	0.103	0.396	0.305
Chest_PCA_7	-0.187	0.079	-2.379	0.023	0.396	0.305

Table B.11: Results of linear regression predicting PASA-Threat with features of head, chest, upper extremities, and total body; β: standardized regression coefficient; σ: standard error; adj.: adjusted

components	β	σ	t	p	R^2	adj. R^2
TotalBody_PCA_1	0.137	0.078	1.755	0.090	0.494	0.337
TotalBody_PCA_2	0.159	0.103	1.539	0.135	0.494	0.337
Chest_PCA_7	-0.268	0.122	-2.206	0.035	0.494	0.337
UpperExtremities_PCA_2	-0.191	0.139	-1.374	0.180	0.494	0.337
UpperExtremities_PCA_5	-0.411	0.138	-2.980	0.006	0.494	0.337
Head_PCA_1	-0.102	0.044	-2.305	0.028	0.494	0.337
Head_PCA_2	0.172	0.081	2.108	0.044	0.494	0.337
Head_PCA_4	-0.104	0.081	-1.285	0.209	0.494	0.337
Head_PCA_7	0.221	0.106	2.075	0.047	0.494	0.337

Appendix C

Acronyms

DBS dried blood spot

CRP c-reactive protein

TSST Trier Social Stress Test

f-TSST friendly Trier Social Stress Test

(f-)TSST TSST or f-TSST

MoCap motion capture

.mvnx MVN open XML format

TUG Timed Up & Go

ECG electrocardiogram

SNS sympathetic nervous system

HPA hypothalamic-pituitary-adrenal

α-amylase alpha-amylase

sAA salivary α-amylase

PASA primary appraisal secondary appraisal

PANAS positive and negative affect schedule

PLD point light display

FACS facial action coding system

FFT fast fourier transform

IC initial contact

TC terminal contact

MS mid stance

SVM support vector machine

PCA principal component analysis

ANOVA analysis of variance

ML machine learning

PANAS-PositiveAffect PANAS positive affect

PANAS-NegativeAffect PANAS negative affect

RFE recursive feature elimination

kNN k-nearest neighbors

CV cross validation

IMU inertial measurement unit

STADI state-trait anxiety-depression inventory

SD standard deviation

IL-6 interleukin-6

SSSQ short state stress questionnaire

SBMLR stepwise backward multiple regression

CoV coefficient of variation

BES Body Esteem Scale

Appendix D

Acknowledgements

I want to thank all study participants, thanks again for participating! Of course I want to thank the whole EmpkinS D03 team for helping me conducting the study (and the memes), which ultimately made this work possible. Additionally, I want to thank all my supervisors, who supported me at all times during this thesis, as well as the *Lab Gang* for making this an awesome time! Thank you for proof reading and of course the emotional support, Annette! Last but not least, I want to say thanks to my family, who supported me starting my studies, even though my motivation in school was fluctuating greatly.